

**Regulation of dendritic MAP2  
mRNA targeting by MARTA2 in  
*Rattus norvegicus***

**Dissertation**

**zur Erlangung des Doktorgrades des  
Fachbereichs Biologie der Universität Hamburg**

vorgelegt von

**KRISHNA H. ZIVRAJ**

**aus DJIBOUTI**

Hamburg 2005

**Regulation of dendritic MAP2  
mRNA targeting by MARTA2 in  
*Rattus norvegicus***

**A dissertation submitted for the fulfillment of  
the requirements for the doctoral degree.**

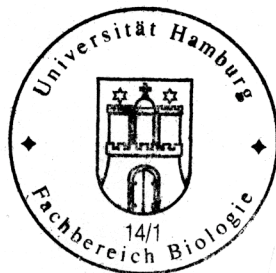
**Faculty of Biology  
University of Hamburg**

By  
**KRISHNA H. ZIVRAJ**  
**from DJIBOUTI**

Hamburg 2005

Genehmigt vom  
Fachbereich Biologie der  
Universität Hamburg  
auf Antrag von Herrn Professor Dr. D. RICHTER  
Weitere Gutachter der Dissertation:  
Herr Professor Dr. H. BRETTING  
Tag der Disputation: 21. Oktober 2005

Hamburg, den 06. Oktober 2005



Professor Dr. Arno Frühwald  
Dekan

## ACKNOWLEDGMENTS

I would like to thank Prof. Dr. Dietmar Richter for giving me the opportunity to do my PhD research in his institute.

Dr. Stefan Kindler, I thank you for being my supervisor, and for your guidance and ideas topped with dollops of encouragement and support.

I would also like to thank Dr. Monika Rehbein for being a guide, as well as a helping hand throughout the course of my PhD work especially for the UV cross-linking assays.

Not forgetting Dr. Hans-Jürgen Kreienkamp, Dr. Evita Mohr and Dr. Dietmar Bächner for all their help and fruitful discussions.

Frau Maria Kienle, I really appreciate your help in all aspects of administrative work.

Many thanks also go to Sönke Harder, Agatha Blaszcyk-Wewer and Dr. Fritz Buck for oligonucleotide synthesis and sequencing.

I am also grateful to Michaela Schweizer from ZMNH for the EM data and special mention to Antonino Schepis from Dr. Krijnse's lab at EMBL, Heidelberg, for providing me with the kinesin dominant negative construct.

I would like to take this opportunity to thank past and present members of our lab: John, Birgit, Christiane, Ricke, Cornelia, Konstanza, Biggi and Hanah, as well as members from other labs in the institute: Chong wee, Gwen, Kerstin, Peter, Katrin, Hans-Hinrich, Nina, Bettina, Jan, Heidje, Stefanie and Hatmone for their help and for creating a very friendly lab atmosphere.

I would like to thank my parents, grandparents, aunts, and my brother and sister for being my backbone and a driving force that allowed me to pursue my goals in life.

And to you Amit, I just say thank you for always being there for me.

## ABBREVIATIONS

<b>°C</b>	degree Celsius
<b>cDNA</b>	complementary DNA
<b>C-terminal</b>	carboxy terminal
<b>CaMKII</b>	calcium/calmodulin-dependent protein kinase II
<b>CPE</b>	cytoplasmic polyadenylation element
<b>CPEB</b>	CPE binding protein
<b>Cy3</b>	Cyanine 3
<b>DIG</b>	dioxygenin
<b>DNA</b>	deoxyribonucleic acid
<b>DTE</b>	dendritic targeting element
<b>EDTA</b>	ethylenediamine tetraacetic acid
<b>EGFP</b>	enhanced green fluorescence protein
<b>ER</b>	endoplasmic reticulum
<b>FBP</b>	FUSE binding protein
<b>FISH</b>	fluorescent <i>in situ</i> hybridization
<b>FUSE</b>	Far upstream binding element
<b>GAPDH</b>	glyceraldehydes-3-phosphate dehydrogenase
<b>GST</b>	glutathione S-transferase
<b>HRP</b>	horseradish peroxidase
<b>IgG</b>	Immunoglobulin G
<b>ISH</b>	<i>in situ</i> hybridization
<b>kDa</b>	kilodalton (s)
<b>KH</b>	K homology domain
<b>M</b>	molarity
<b>MAP2</b>	microtubule associated protein 2
<b>MARTA</b>	MAP2 mRNA trans-acting factor
<b>mRNA</b>	messenger ribonucleic acid
<b>min</b>	minute (s)
<b>mol</b>	mole(s)

<b>MBP</b>	myelin basic protein
<b>N-terminal</b>	amino terminal
<b>nt</b>	nucleotide
<b>NLS</b>	nuclear localization signal
<b>PCR</b>	polymerase chain reaction
<b>RNA</b>	ribonucleic acid
<b>RNase</b>	ribonuclease
<b>RNP</b>	ribonucleoprotein
<b>RSW</b>	ribosomal salt wash
<b>RT</b>	room temperature
<b>s</b>	second
<b>SCG</b>	superior cervical ganglia
<b>TAE</b>	Tris-(hydroxymethyl)-aminomethane
<b>Tris</b>	2-amino-2(hydroxymethyl)-1,3-propanediol
<b>U</b>	unit (s) of enzyme activity
<b>UTR</b>	untranslated region
<b>UV</b>	ultraviolet
<b>VLE</b>	Vg1 localization element
<b>v/v</b>	volume per volume
<b>w/v</b>	weight per volume
<b>ZBP</b>	zipcode binding protein

---

**Table of Contents**

<u>Chapter</u>	<u>Content</u>	<u>Page</u>
1	Introduction	
1.1	RNA localization in eukaryotic cells	1
1.1.1	<i>Cis</i> -acting targeting elements	5
1.1.2	<i>Trans</i> -acting factors	6
1.1.3	Cytoskeletal elements and motor proteins	8
1.2	Purpose of this study	9
2	Materials and Methods	
2.1	Materials	12
2.1.1	Plasmids and oligonucleotides	12
2.1.1.1	Basic plasmid vectors	12
2.1.1.2	Constructed vectors	12
2.1.1.3	Oligonucleotides	14
2.1.2	Antibodies	15
2.1.3	Microbial strains and lab animals	16
2.1.4	Chemicals	16
2.2	Methods	16
2.2.1	Molecular biology techniques	16
2.2.1.1	Polymerase chain reaction (PCR)	16
2.2.1.2	Restriction endonuclease digestion of DNA samples, agarose gel electrophoresis and DNA purification	17
2.2.1.3	DNA ligation, transformation and plasmid purification	18
2.2.1.4	Nucleic acid concentration	18

---

	determination and DNA sequencing	
	2.2.1.5 RNA isolation and cDNA synthesis	19
	2.2.1.6 <i>In vitro</i> synthesis of digoxigenin-labeled probes	19
	2.2.1.7 Dot-blot quantification	19
2.2.2	Biochemical techniques	20
	2.2.2.1 SDS-polyacrylamide gel electrophoresis (SDS-PAGE)	20
	2.2.2.2 Western blot analysis	20
	2.2.2.3 Subcellular fractionation of rat brain homogenate, affinity purification of antibodies and immunoprecipitation	21
	2.2.2.4 Ultraviolet cross-linking assay	22
2.2.3	Cell biology techniques	22
	2.2.3.1 Preparation and transfection of primary hippocampal neurons	22
	2.2.3.2 Immunocytochemistry and <i>in situ</i> hybridization in primary neurons	23
	2.2.3.3 Detergent extraction for primary neurons	24
	2.2.3.4 Immunogold labeling in tissue sections	25
	2.2.3.5 Microscopy and quantification	25
3	Results	27
3.1	Dendritic distribution of MAP2 mRNA in cultured neurons	27
3.1.1	Targeting of MAP2 mRNA into dendrites is an early event during neuronal differentiation	27

---

3.2	Characterization of the MAP2 mRNA <i>trans</i> -acting factor	32
	MARTA2	
3.2.1	Generation of antibodies against MARTA2	32
3.2.2	Subcellular distribution of MARTA2 in the adult rat brain	36
3.2.3	MARTA2 distribution in cultured hippocampal neurons	38
3.2.4	MARTA2 fusion proteins mimic endogenous MARTA2 distribution in neurons	41
3.2.5	MARTA2 is associated with the cytoskeleton	43
3.2.6	MARTA2 resides in somata and dendrites of rat brain neurons	45
3.3	Functional characterization of MARTA2	47
3.3.1	Endogenous and recombinant MARTA2 co-localize with endogenous MAP2 mRNA <i>in situ</i>	47
3.3.2	Over-expression of truncated MARTA2 disrupts dendritic targeting of MAP2 mRNA	50
3.3.3	MARTA2-KH-EGFP has no significant effect on the total mRNA pool	55
3.3.4	Kinesin I mediates transport of MAP2 mRNA granules into dendrites	57
4	Discussion	60
5	Summary	69
6	References	70

## **CHAPTER 1: INTRODUCTION**

### **1.1 RNA localization in eukaryotic cells**

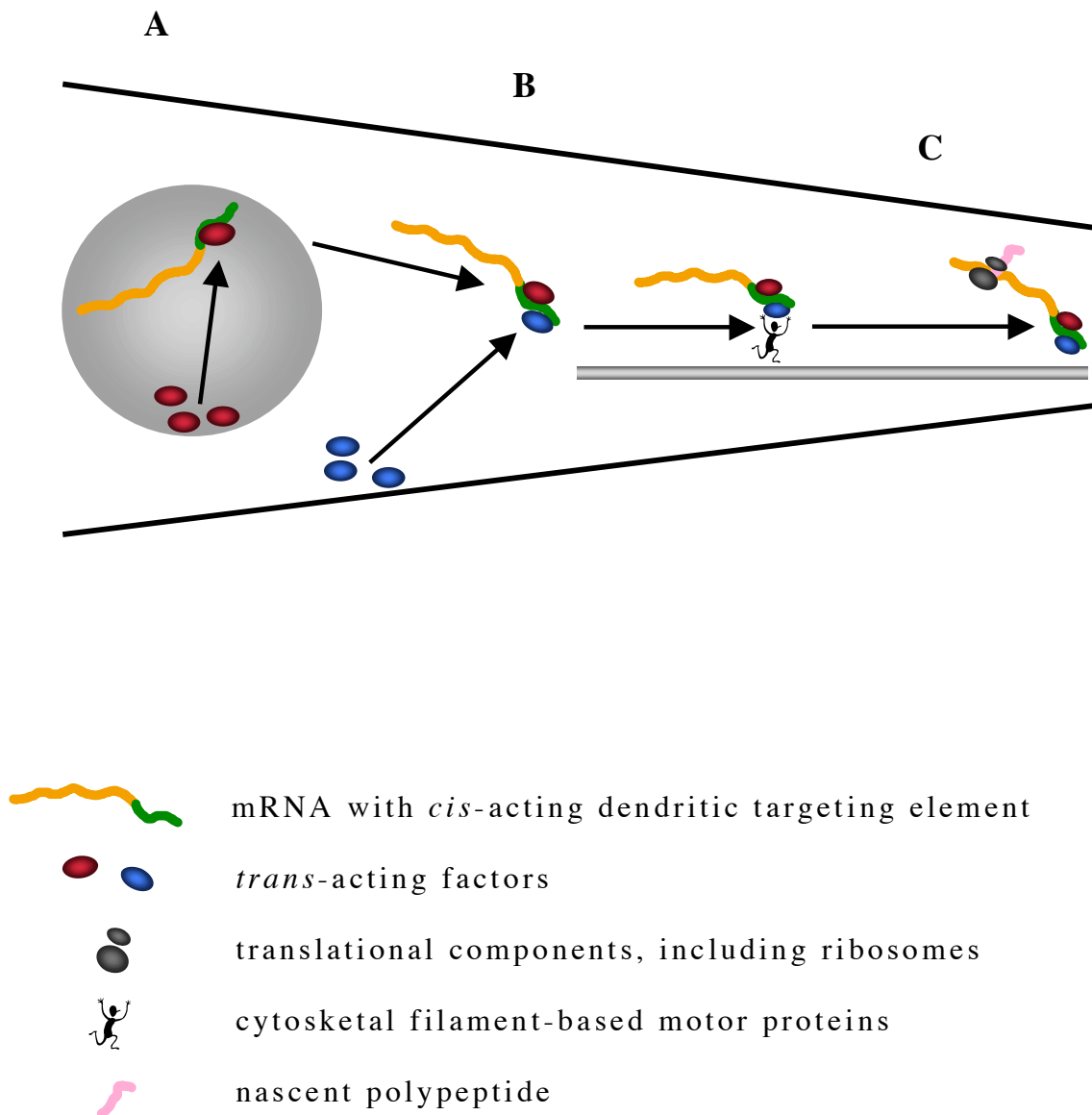
Cytoplasmic RNA localization is an evolutionary conserved mechanism that contributes to spatially restricted protein synthesis. The first hint on RNA localization in eukaryotic cells dates back to the 1960s when ribosomes associated to endoplasmic reticulum (ER), together known as “ergastoplasm”, were detected near synapses in spinal cord neurons of monkeys by electron microscopy (Bodian 1965). This anatomical finding suggested that these neurons employed protein synthesis of localized RNAs for their synaptic function. Several years later, the concept of RNA localization was established not only in neurons but also in various other cell types ranging from unicellular organisms such as yeasts, to oocytes and embryos of *Drosophila*, *Xenopus*, ascidians and echinoderms. In fact, the *Xenopus* oocyte was the first system in which maternally synthesized, cytoplasmically localized RNAs were identified (Rebagliati *et al.* 1985). However, it was in the *Drosophila* oocyte and embryo where the localization of the maternal bicoid RNA to the anterior pole was shown to be functionally important for the normal development of the embryo (Frigerio *et al.* 1986; Berleth *et al.* 1988). The discovery of an actual function for bicoid RNA localization in specification of anterior cell polarity during *Drosophila* embryonic development motivated researchers to study this process in great detail. The role of RNA localization was subsequently deciphered in many cell systems. One of the main reasons why RNA is localized to a specific cell region is to produce a high concentration of protein in the given cell area (Kloc *et al.* 2002). This function is evident in motile fibroblasts in which  $\beta$ -actin mRNA is localized to the leading

edge to produce high amounts of  $\beta$ -actin protein (Kislauskis *et al.* 1994; Ross *et al.* 1997). RNA localization is also important in establishing morphogen gradients as seen in the *Drosophila* embryo. The localization of bicoid RNA to the anterior pole and nanos RNA to the posterior pole of the fly embryo leads to concentration gradients of bicoid and nanos proteins necessary for specifying cell polarity (Bashirullah *et al.* 1998). Similarly, in *Xenopus* oocytes, Vg1 RNA localization to the vegetal pole underlies the animal-vegetal axis formation during *Xenopus* oogenesis (Palacios and St Johnston 2001). The localization of ASH1 RNA to the tip of budding yeast cells regulates mating type switching (Long *et al.* 1997). And lastly, in mammalian neurons, several RNAs are targeted to processes where their local translation appears to be modulated by synaptic activity (Bodian 1965; Steward and Levy 1982; Aranda-Abreu *et al.* 1999; Aronov *et al.* 2002).

### **Mechanisms of RNA localization**

Current understanding of the mechanism by which localized mRNAs are targeted to their final destinations involves recognition of *cis*-acting RNA elements, by *trans*-acting RNA binding factors (Kindler *et al.* 2005). *Cis*-acting elements are regions within a given RNA, containing codes specific for localization. Such codes are recognized by RNA-binding *trans*-acting factors and together they form ribonucleoprotein (RNP) complexes. These RNP complexes reach their final destination with the help of motor proteins moving along cytoskeletal filaments (Guzik and Goldstein 2004; Hirokawa and Takemura 2005). RNP complexes can form within the nucleus and travel outside into the cytoplasm where they may get remodeled and additional transport factors may get recruited. Evidence for the formation of RNP complexes in the nucleus comes from *Drosophila* and *Xenopus*. In fly oocytes, splicing at the first

exon-junction of oskar mRNA in the nucleus for instance, is essential for oskar mRNA localization at the posterior pole suggesting that nuclear events are mechanistically coupled with cytoplasmic RNA localization (Hachet and Ephrussi 2004). Similarly, in *Xenopus* oocytes, the vegetal localization of Vg1 mRNA involves recognition of the transcript by *trans*-acting factors in the nucleus, and the formation of specific RNP complexes that are eventually exported out into the cytoplasm (Kress *et al.* 2004). Moreover, some of the identified *trans*-acting RNA-binding proteins have a nuclear distribution implying that these proteins may serve as nucleocytoplasmic shuttling proteins that regulate nuclear and cytoplasmic mRNA targeting. Zipcode binding protein 2 (ZBP2) is one such example of a predominantly nuclear protein that regulates cytoplasmic localization of  $\beta$ -actin mRNA (Gu *et al.* 2002). Figure 1 summarizes the mechanism of RNA localization by a diagrammatic representation of a mammalian neuron in which dendritic mRNA localization is of prime importance in synaptic protein synthesis.

**FIGURE 1**

**Cytoplasmic mRNA localization exemplified by dendritic RNA targeting in neurons.** (A) Recognition of RNA *cis*-acting elements (green) by *trans*-acting factors (red eclipses) in the nucleus forming RNP complexes. (B) Nuclear export of RNP particles into the soma and recruitment of additional *trans*-acting factors (blue eclipses) into the complex. (C) Transport of the remodeled RNP complex along cytoskeletal filaments (grey line) with the help of motor proteins to the dendrite where components of the translational machinery such as ribosomes (grey eclipses) attach to the RNP complex to start local protein synthesis. Ribosomes may even attach to the RNP complex and travel with it before reaching the target site.

### 1.1.1 Cis-acting targeting elements

*Cis*-acting elements have been identified for a number of mRNA transcripts in various cell systems. In *Xenopus* oocytes for instance, localization of Vg1 mRNA to the vegetal pole during oogenesis is mediated by a 340-nucleotide sequence termed Vg1 localization element (VLE) (Mowry and Melton 1992). Similarly, dendritic targeting elements (DTEs) have been identified for a number of dendritically localized mRNAs. DTEs of different RNAs appear to be distinct in length and sequence. This complex nature of the DTEs may account for the diversity of the target sites of various mRNAs within a given dendrite (Kindler *et al.* 2005). In addition to variations in sequence and length among the different DTEs, some mRNAs also contain multiple *cis*-acting elements. Calcium/calmodulin-dependent protein kinase II (CaMKII) mRNA is a dendritically localized RNA whose 3' untranslated region (3'UTR) contains three distinct non-overlapping DTEs: a 30-nucleotide long sequence (Mori *et al.*, 2000), a 1200-nucleotide stretch in the 3'UTR (Blichenberg *et al.* 2001) and two copies of a hexanucleotide motif called the cytoplasmic polyadenylation element (CPE) (Huang *et al.* 2003). Transcripts encoding the microtubule-associated protein 2 (MAP2), a protein that is important for cytoskeletal stability, contain a 640-nucleotide DTE in its 3'UTR (Blichenberg *et al.* 1999). On the other hand,  $\beta$ -actin mRNA contains only a 54-nucleotide *cis*-acting element termed as the “zipcode” (Eom *et al.* 2003). In addition to unique *cis*-acting elements, there are some common motives such as the 11-nucleotide heterogeneous ribonucleoprotein element (hnRNP) A2 response element (A2RE). Targeting of myelin basic protein (MBP) mRNA in oligodendrocytes is mediated by A2RE (Carson *et al.* 2001). A2RE also mediates extrasomatic trafficking of human

immunodeficiency virus 1 (HIV-1) in cultured oligodendrocytes (Mouland *et al.* 2001). Hence, localized mRNAs make use of unique and shared *cis*-acting elements to mediate transport to the RNA's final destination.

### 1.1.2 **Trans-acting factors**

*Trans*-acting factors are RNA-binding proteins that mediate RNA localization by interacting with *cis*-acting elements. The most well studied *trans*-acting proteins consist of either RNA recognition motifs (RRMs) or hnRNP K homology (KH) domains, or a combination of both (Bassell and Kelic 2004). Vg-1 RNA binding protein (Vg1RBP) or Vera and zipcode binding protein 1 (ZBP1) are examples of such *trans*-acting proteins that bind to Vg1-VLE and  $\beta$ -actin zipcode, respectively (Deshler *et al.* 1997; Zhang *et al.* 2001; Eom *et al.* 2003; Tiruchinapalli *et al.* 2003). Another family of *trans*-acting factors is the FUSE-binding protein (FBP) family comprising of three homologous members (Davis-Smyth *et al.* 1996). One member of the family namely FBP1, binds to the far-upstream element (FUSE) of the human *c-myc* oncogene, and is involved in transcriptional regulation (Duncan *et al.* 1994). All three family members are characterized by the presence of four central KH-domains that bind to single-stranded DNA/RNA (Braddock *et al.* 2002). Figure 2 shows the domain structure of the three members of the FBP family, FB1, FBP2 and FBP3. The KH domains were first identified and characterized in hnRNPK (Siomi *et al.* 1994). MAP2 RNA trans-acting factors 1 and 2 (MARTA1 and MARTA2) are rat orthologs of FBP2 and FBP3, respectively. These two *trans*-acting proteins were identified by ultraviolet (UV) cross-linking assays to bind to the DTE of MAP2 mRNA with nanomolar affinities (Rehbein *et al.* 2000).

## FUSE-BINDING PROTEIN FAMILY

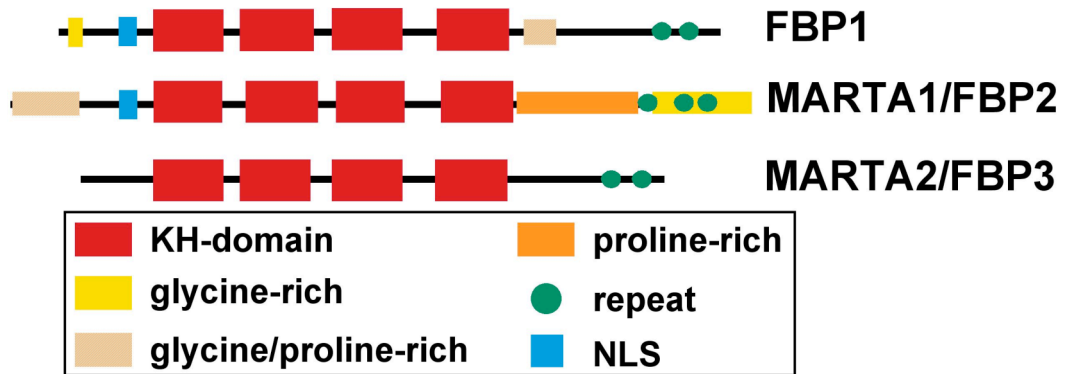


**FIGURE 2**

**Domain structure of members of the FUSE-binding protein family FBP1, MARTA1/FBP2 and MARTA2/FBP3.** The four central KH domains (red squares) are present in all three members along with the tyrosine rich C terminus (green circles). In contrast to FBP3, FB1 and FB2 have a nuclear localization sequence (NLS) shown as blue boxes. In addition to the NLS, both FBP1 and 2 have glycine-rich (yellow boxes) and glycine/proline-rich amino acid stretches. Furthermore, MARTA1/FBP2 has an additional proline-rich region (orange rectangle) before the tyrosine repeats. (Figure adapted from Davis-Smyth *et al.*, 1996).

MARTA1/FBP2 also known as KH-type splicing regulatory protein (KSRP) is involved in mRNA splicing (Min *et al.* 1997). ZBP2, the chicken ortholog of MARTA1 binds to the zipcode of  $\beta$ -actin mRNA and plays a role in targeting  $\beta$ -actin mRNA to growth cones of neurons in culture (Gu *et al.* 2002). Moreover, recent work by (Gherzi *et al.* 2004) has shown a role of KSRP in RNA degradation pathway. While the functional significance of FBP2/KSRP/ZBP2 in mRNA processing and localization is relatively well characterized, the exact function of FBP3/MARTA2 remains unknown (Davis-Smyth *et al.* 1996). However, the fact that FBP3/MARTA2 belongs to the FBP family comprising of highly related proteins raises the possibility that FBP3/MARTA2 may also play a role in RNA processing and transport.

The above listed *trans*-acting factors are involved in RNA localization. However, there are other RNA-binding proteins that are involved in RNA trafficking as well as in translational control. The Staufen family of double-stranded (ds) RNA-binding proteins is a classic example of such proteins. *Drosophila* Staufen is shown to be essential for the localization and translational control of different maternal RNAs that specify the anterior-posterior polarity (Roegiers and Jan 2000). Two orthologs of Staufen, namely Stau1 and Stau2 have been described in mammals. In neurons, both Stau1 and Stau2 are present in dendrites as granules. Furthermore, both proteins are enriched in polysome fractions suggesting their role in translational regulation (Monshausen *et al.* 2001; Tang *et al.* 2001; Duchaine *et al.* 2002). Recently purified Staufen1-RNP complexes showed that the protein might interact directly with the ribosomal protein P0 which forms the P-stalk of the ribosome (Brendel *et al.* 2004). Similarly, cytoplasmic polyadenylation element binding protein (CPEB) that binds to the *cis*-acting CPE element also has the dual function of RNA localization and translational control. CPEB mediates both cytoplasmic polyadenylation-induced translation and transport of CPE-containing mRNAs to dendrites (Huang *et al.* 2003). Thus, unique as well as conserved *trans*-acting RNA binding proteins regulate RNA transport and in many cases also control translation of the mRNA.

### **1.1.3 Cytoskeletal elements and motor proteins**

Specific interactions between *cis*-acting elements and *trans*-acting factors result in the formation of RNP complexes, which need to be transported along the cell cytoskeleton to reach the target site. While microfilaments are used to localize  $\beta$ -actin RNA along with ZBP1 in fibroblasts, the same RNA-protein

complex predominantly travels along microtubules in neurons (Bassell and Kelic 2004). Both kinesin and dynein motors are involved in RNA transport along microtubules (Guzik and Goldstein 2004; Hirokawa and Takemura 2005). Neuronal CPEB granules for example, contain both kinesin and dynein as motor proteins thereby allowing bidirectional movement along microtubules (Huang *et al.* 2003). Several RNA-binding proteins that function as *trans*-acting factors have been recently identified as components of conventional kinesin complexes (Kanai *et al.* 2004). Hence, molecular motors in RNA transport particularly in neurons are important components that facilitate RNP complexes to traverse long distances along the cell cytoskeleton to reach its final destination.

## **1.2 Purpose of this study**

mRNA localization is by now a well-documented process for post-transcriptional gene regulation and selective protein sorting mainly based on studies in *Drosophila* and *Xenopus* oocytes (Palacios and St Johnston 2001; Kindler *et al.* 2005). In the mammalian brain, the first mRNA found to be localized in dendrites encodes MAP2. The mRNA was detected by radioactive *in situ* hybridization (ISH) in the molecular layers of the hippocampus and in the neocortex of the developing rat brain (Garner *et al.* 1988). In contrast, transcripts encoding other cytoskeletal proteins like  $\beta$ -tubulin are restricted to neuronal somata (Bruckenstein *et al.* 1990; Kleiman *et al.* 1990). MAP2 being the most abundant MAP in the mammalian brain is exclusively found in somata and dendrites but not in axons (Caceres *et al.* 1984; Caceres *et al.* 1984). The protein is important for the cytoskeletal organization as it is involved in microtubule assembly and stabilization in dendrites (Goedert *et al.* 1991; Matus 1994). Evidence for its role in defining dendrite

morphology and stability came from MAP2 deficient mice that showed an impairment of dendrite elongation (Harada *et al.* 2002). Hence, with the discovery of MAP2 mRNA in dendrites, it became important to decipher the components involved in the selective targeting of this particular mRNA in neurons. The identification and characterization of the *cis*-acting DTE in the 3'UTR of rat MAP2 mRNA was a major step forward in identifying the individual players mediating its dendritic targeting (Blichenberg *et al.* 1999)

Although, two rat *trans*-acting factors namely MARTA1 and MARTA2 have been identified as specific DTE-binding proteins in UV cross-linking assays (Rehbein *et al.* 2000), it still remains to be shown whether these proteins play a role in dendritic targeting of MAP2 mRNA in neuronal cells. Focusing on MARTA2, it was previously shown that the protein is strongly enriched in ribosomal salt wash (RSW) fractions obtained from the adult rat brain (Rehbein *et al.* 2000). RSW fractions contain components of dissociated RNP complexes and translational initiation factors (Merrick 1992). MARTA2 was recently affinity purified from RSW proteins of the adult rat brain (Zivraj *et al.* 2005), and, the aim of the current study is to functionally characterize MARTA2 and study its role in the regulation of dendritic MAP2 mRNA trafficking in rat neurons.



## **CHAPTER 2: MATERIALS AND METHODS**

### **2.1 MATERIALS**

#### **2.1.1 Plasmids and oligonucleotides.**

##### **2.1.1.1 Basic plasmid vectors.**

The following plasmids were used for cloning of PCR products and for construction of prokaryotic and eukaryotic expressing vectors. Accession numbers are also provided.

<b>Plasmid</b>	<b>Source</b>	<b>Accession number</b>
pBluescript SK II (+)	Stratagene	X52328
pEGFP-N1, N3	Clontech	U55762, U57609
pEYFP-C1	Clontech	U55763.
pGEX-6P-3	Amersham Biosciences	U78874

**Table 1:** Commercially available basic prokaryotic and eukaryotic expressing vectors. Sequences of the corresponding vectors are available at GenBank ([www.ncbi.nlm.nih.gov](http://www.ncbi.nlm.nih.gov)) through their accession numbers listed above as well as from their respective sources.

##### **2.1.1.2 Constructed vectors.**

Below are lists of eukaryotic expression vectors constructed for this study. Also listed is prokaryotic and eukaryotic expression vectors obtained from colleagues in the laboratory as well as from other laboratories. In addition, vectors used for *in vitro* transcription are also provided.

**A) Eukaryotic expression vectors constructed for the study:**

<b>Vector name</b>	<b>Basic vector</b>	<b>Accession # &amp; nucleotide length.</b>	<b>Oligonucleotide used for PCR</b>	<b>Cloning sites</b>
<b>pMARTA2-EGFP</b>	pEGFP-N3	DQ144645 nt 1-1710	20s and 21as	XhoI, KpnI
<b>pMARTA2-KH-EGFP</b>	pEGFP-N3	DQ144645 nt 211- 1281	22s and 23as	XhoI, KpnI
<b>pCPEB-EGFP</b>	pEGFP-N3	XM_218858 nt 1- 2614	CPEB-sense & CPEB-as	XhoI, KpnI

**B) Prokaryotic and eukaryotic expression vectors from laboratory colleagues and other laboratories:**

<b>Vector name</b>	<b>Basic vector</b>	<b>Source</b>	<b>Accession # &amp; nucleotide length</b>
<b>pN-MARTA2-GST</b>	pGEX-6P-3	Dr. Rehbein, Dr. Kindler's lab, Hamburg.	DQ144645, nt 1-310
<b>pC-MARTA2-GST</b>	pGEX-6P-3	Dr. Rehbein, Dr. Kindler's lab, Hamburg	DQ144645, nt 1270-1710
<b>pEYFP-MARTA2</b>	pEYFP-C1	Dr. Rehbein, Dr. Kindler's lab, Hamburg	DQ144645, nt 1-1710
<b>truncated Staufen2-EGFP</b>	pEGFP-N1	Dr. Brendel, Dr. Kindler's lab, Hamburg	NM_001007149, nt 178-1746
<b>pdnKin1-EGFP</b>	Home made plasmid from Dr. Krijnse's lab.	Antonino Schepis, Dr. Krijnse's lab, EMBL, Heidelberg	XM_341538, nt 18- 990

<b>pDyn-EGFP</b>	pEGFP-N1	Prof. Vallee's lab, NM_006400, Columbia University, USA.	nt 133-1353
------------------	----------	---	-------------

**C) Vectors used for in vitro transcription of RNA probes:**

<b>Vector name</b>	<b>Basic vector</b>	<b>Source</b>	<b>Acession # &amp; nt length</b>
<b>pBS-MAP2-sense</b>	pBS-SK II (+)	Dr. Kindler, Hamburg.	X51842, nt 60-5552
<b>pBS-MAP2-antisense</b>	pBS-SK II (+)	Dr. Kindler, Hamburg.	X51842, nt 60-5552
<b>pBS- <math>\beta</math>-Tubulin</b>	pBS-SK II (+)	Dr. Rehbein, Dr. Kindler's lab, Hamburg.	NM_022298, nt 1-1600

**2.1.1.3 Oligonucleotides**

All oligonucleotides listed below were synthesized at the service-laboratory in the Institute for Cell Biochemistry and Clinical Neurobiology (University Hospital Eppendorf, Hamburg) with a DNA/RNA Synthesizer (Applied Biosystems). The oligonucleotides were dissolved in sterile water and purified over MICROSPIN G-25 columns (Amersham Biosciences) following the manufacturer's instructions. Oligonucleotide concentration was determined as described in (2.2.1.4) and diluted to 10 pmol/ $\mu$ l for subsequent usage in PCR reactions.

<b>Name</b>	<b>Sequence</b>	<b>Restriction sites</b>
20 s	5'- AAA <u>CTC GAG</u> CCA CCA TGG CGG AGC TGG TG- 3'	Xho1
21 as	5'- AAA <u>GGT ACC</u> CTG CTC CTG GCT GTG.GG- 3'	Kpn1
22 s	5'- AAA <u>CTC GAG</u> CCA CCA TGG TAC	Xho1

	ATC AAA GGG CAG TA- 3'	
23 as	5'- AAA <u>GGT ACC</u> GCC AAC TTT CTC ATC TAT- 3'	Kpn1
CPEB- sense	5'- AAA <u>CTC GAG</u> <b>CCA CCA</b> TGC TTT TCC CCA CCT CTG- 3'	Xho1
CPEB-as	5'- AAA <u>GGT ACC</u> GTT CTT CTG GTCC CCT CAT TAG- 3'	Kpn1

**Table 2 List of oligonucleotides used for PCR amplification.** Underlined nucleotides represent restriction enzyme site. Shaded in grey is the Kozak sequence and letters in bold show the ATG start codon.

### 2.1.2 Antibodies.

Primary antibody	Working Concentration		Source
	Western blot	Immunocytochemistry	
m anti-dig-Cy3	-	1:100	Dianova
m anti-GAPDH	-	1:800	Ambion
m anti-MAP2	-	1:1000	Sigma
rb anti-GFP	1:10000	1:1000	Abcam
rb anti-MAP2	-	1:2000	Dr. Garner, Stanford University, USA
rb anti-MARTA2-N54, C98 & C99.	1:1000	1:100	Our laboratory

Secondary antibody	Working Concentration		Source
	Western blot	Immunocytochemistry	
g-anti-rb-Alexa Fluor ® 488	-	1:500	Invitrogen
g-anti-m-Alexa Fluor ® 546	-	1:500	Invitrogen
g-anti-rb-Marina Blue	-	1:500	Invitrogen

---

g-anti-m-Cyanine3 <sup>TM</sup> -	1:100	Dianova
HRP-anti-rbIgG	1:10000 -	Amersham Biosciences

---

**Table 3:** Antibodies used for Western blot and immunocytochemical analysis with their working concentration for each assay. The species origin of the immunoglobulin is indicated by the abbreviation at the start and in the middle of each antibody name; g = goat, rb = rabbit, m = mouse.

### **2.1.3 Microbial strains and lab animals.**

---

	<b>Name</b>	<b>Source</b>
<b>Bacterial strain</b>	<i>E.coli</i> XL1 blue	Stratagene
<b>Laboratory animal</b>	<i>Rattus norvegicus</i> (Wistar-rat)	Animal facility at University Clinic Eppendorf (UKE).

---

### **2.1.4 Chemicals.**

All chemicals of analytical grade were purchased from Fluka, Merck, Sigma, Roth and Tocris unless otherwise stated.

## **2.2 METHODS**

### **2.2.1 Molecular Biology techniques**

#### **2.2.1.1 Polymerase chain reaction (PCR)**

All PCR reactions were performed with Master mix (Qiagen) containing Taq DNA polymerase in a GeneAmp PCR System 2400 Thermocycler (Perkin Elmer). The reaction components and conditions of individual reactions are shown below:

<b>Reaction components</b>	<b>Amount</b>	
DNA template	10-200 ng	
Forward primer (10 pmol/ $\mu$ l)	3 $\mu$ l	
Reverse primer (10 pmol/ $\mu$ l)	3 $\mu$ l	
2x Master mix	25 $\mu$ l	
Sterile water	to bring to a final volume of 50 $\mu$ l	

	<b>Temperature and time</b>	<b># cycles</b>
Initial denaturation	94°C, 5 min	
Denaturation	94°C, 30 s	35 cycles
Annealing	53-55°C, 30 s	35 cycles
Extension	72°C, 1 min/kb of the desired PCR product.	35 cycles
Final extension	72°C, 10 min 4°C, pause	

An aliquot of each PCR reaction was analyzed by gel electrophoresis and PCR products were purified (2.2.1.2) for subsequent experiments. The purified PCR products that have an A tail at their 3' ends was cloned into the pGEM®-T Easy Vector system (Promega). The reactions were performed according to the manufacturer's protocol.

### **2.2.1.2 Restriction endonuclease digestion of DNA samples, Agarose gel electrophoresis and DNA purification**

(Sambrook *et al.* 1989)

Restriction endonuclease digestions of DNA samples were performed as recommended by the manufacturers (Invitrogen and New England Biolabs). Digested samples were analyzed via agarose gel electrophoresis (Sambrook *et al.* 1989). Gene

Ruler™ 100bp DNA ladder (MB1 Fermentas) was used as molecular weight marker. The gel was electrophoresed in 1x TAE buffer at a constant voltage of 80-100 volts and was then viewed and photographed under ultraviolet light from a UV transilluminator (UVT- 28M, Herolab) with Digi-Cam Olympus C-740 camera. DNA fragments were purified from agarose gel using QIAEX II Agarose Gel Extraction Kit or PeQLab Gel Extraction Kit according to the manufacturer's instructions.

#### **2.2.1.3 DNA ligation, transformation and plasmid purification**

For ligation, digested inserts and linearized vectors were mixed in an approximate 3:1 molar ratio. One unit of T4 DNA ligase (Roche) and a final concentration of 1x ligase buffer were added to the ligation mixture. Ligation was carried out at room temperature for 3 hours. DNA transformation was done in XL1 Blue *E.coli* competent cells (Stratagene) following the manufacturer's recommendation. Small and large-scale plasmid preparations were performed with FastPlasmid-mini columns (Eppendorf) and Nucleobond® AX Kit (Macherey and Nagel) kits, respectively, as described in the manufacturers' guidebooks. Endotoxin-free DNA that was used for transfection of primary hippocampal neurons was prepared with Endo-free maxi kits (Qiagen) as per the manufacturer's recommendation.

#### **2.2.1.4 Nucleic acid concentration determination and DNA sequencing**

Nucleic acid concentration was determined with the spectrophotometer Genequant (Amersham Biosciences) as described by Sambrook et al., (1969). All DNA sequencing reactions were done in the sequencing service laboratory of Institute for Cell Biochemistry and Clinical Neurobiology, UKE,

Hamburg according to the Dideoxy methodology (Sanger *et al.* 1977).

### **2.2.1.5 RNA isolation and cDNA synthesis**

RNA was isolated from adult rat brain by homogenizing the tissue in Trizol (Invitrogen) as per the manufacturer's recommendation. Isolated RNA was used for reverse transcription with SUPERScript II (Invitrogen) to generate cDNA following the manufacturer's guidelines.

### **2.2.1.6 In vitro synthesis of digoxigenin-labeled probes**

pBS-MAP2 plasmids containing the MAP2 sequence in both orientations were linearized with SmaI, and sense and antisense digoxigenin (DIG)-labeled riboprobes were transcribed with T7 polymerase according to the manufacturer's description (Roche, Boehringer Mannheim). pBS- $\beta$ -Tubulin was linearized with either ClaI or XbaI and T3 and T7 RNA polymerases (MB1 Fermentas) were used to transcribe DIG-labeled sense and antisense riboprobes, respectively. For the detection of poly(A) RNA, oligo d(T)<sub>50</sub> was end-labeled with DIG-UTP (Roche) as recommended. In control experiments, the same probe was used in the presence of a 100-fold excess of unlabeled oligo d(T)<sub>50</sub>. The riboprobes were purified as described (Blichenberg *et al.* 1999).

### **2.2.1.7 Dot blot quantification**

To estimate the yield of DIG-labeled RNA probes, dot blot quantification was performed. First, 1  $\mu$ l spots of a series of dilutions of newly-labeled probes and a probe of known concentration were applied to a strip of Hybond-XL membrane (Amersham Biosciences). The membrane was cross-linked with UV light in a UV cross-linker (Stratagene) using the automated program. The membrane was washed briefly in buffer 1 (100 mM

Tris-HCl pH 7.5, 150 mM NaCl) and blocked in 1% blocking reagent (Boehringer Mannheim) in buffer 1 for 30 min at RT. The membrane was then incubated with alkaline phosphatase conjugated-sheep anti-Digoxigenin antibody (Roche) in blocking buffer for 1 hour at RT followed by incubation with the color substrate solution (45  $\mu$ l nitroblue tetrazolium (NBT) and 35  $\mu$ l 5-bromo-4-chloro-3-indolyl phosphate (BCIP) in 100 mM Tris-HCl pH 9.5, 100 mM NaCl, 50 mM  $MgCl_2$ ). The color reaction was performed in the dark and once the RNA probe spots appeared on the membrane, the reaction was stopped with sterile water.

## **2.2.2 Biochemical techniques**

### **2.2.2.1 SDS-Polyacrylamide gel electrophoresis (SDS-PAGE)**

(Laemmli 1970)

SDS-PAGE gels containing 10-12% polyacrylamide in the separation gel and a stacking gel, cast according to Laemmli's methodology (1970), were used for protein separation. Concentration of all protein samples was determined using the Bradford reagent (Sigma) (Bradford, 1976). Ten to forty  $\mu$ g of proteins denatured at 95°C in 1x Laemmli buffer (Laemmli, 1970) for 5 minutes were loaded per well. Electrophoresis was performed at 150-200 V in 1x SDS running buffer (25 mM Tris-base, 19.2 mM glycine, 0.1% (w/v) SDS). Molecular weight of the proteins was estimated with the protein molecular weight marker (Full Range Rainbow Marker, Amersham Biosciences), which was run alongside with the protein samples.

### **2.2.2.2 Western blot analysis**

Proteins separated in an SDS-PAGE were electro-transferred and immobilized onto nitrocellulose membrane

(PROTRAN, Schleicher & Schuell) in blotting buffer (38 mM glycine, 47 mM Tris, 0.03% (v/w) SDS, 20% methanol) in a semi-dry transfer blot apparatus (SEMIDRY, BioRad) for 30 min at 10-15 V. The membrane was incubated for 1 hour with blocking buffer (5% (w/v) skim milk powder in PBS-T; PBS: 137mM NaCl, 8.8 mM Na<sub>2</sub>HPO<sub>4</sub>, 2.7 mM KCl, 0.7 mM KH<sub>2</sub>PO<sub>4</sub>, pH 7.4; PBS-T: PBS, 0.1% Tween-20). The membrane was then incubated with the appropriate primary antibody diluted in blocking buffer overnight at 4°C. The membrane was then washed thrice with PBS-T (10 min/wash) followed by incubation with appropriate HRP (horse raddish peroxidase)-conjugated secondary antibody diluted in blocking buffer for 1 hour at RT. The membrane was washed as before and the luminescence signal generation was done with ECL™ (Enhanced Chemiluminescence, Lumi-Light Western Blotting Substrate, Roche). Chemiluminescence signals were detected on a Cronex 5 Medical X-Ray Film (Agfa). For the blocking experiment, affinity purified MARTA2 antisera N54, C98 and C99 were pre-incubated with 2 µg/mL of MARTA2-GST fusion proteins in 10% normal goat serum (NGS) in PBS, overnight at 4°C. The blocked antisera were then used as primary antibodies for western blot analysis.

### **2.2.2.3 Subcellular fractionation of rat brain homogenate, affinity-purification of antibodies and immunoprecipitation**

Rat brain crude lysate and the different subcellular fractions namely the nuclear, S100, polysomes and RSW fractions were prepared following the detailed methodology provided by Rehbein *et al.* (2000). Antibody affinity-purification was essentially performed as described (Monshausen *et al.* 2002). For immunoprecipitation, crude lysate was incubated with 3 µl affinity purified rabbit MARTA2-C98 antiserum and 20 µl Protein A Agarose

suspension (Santa Cruz Biotechnology) pre-washed with IP buffer (50 mM Tris-HCl pH 8.0, 120 mM NaCl, 0.5% NP40, 1 mM EDTA, 4% (v/v) proteinase inhibitor cocktail [Roche]) at 4°C overnight in a rotor. The agarose beads were washed five times with IP buffer and resuspended in Laemmli buffer followed by Western blot analysis.

#### **2.2.2.4 Ultraviolet cross-linking assay**

Ultraviolet cross-linking assay was done as described (Rehbein *et al.* 2002). Immunoprecipitation of MARTA1 and MARTA2 after UV cross-linking to the MAP2-DTE probe, was essentially carried out as described (Rehbein *et al.* 2002). In brief, for each 50 µl reaction, 10 µg protein from a RSW fraction were incubated with 20 fmoles MAP2-DTE probe, cross-linked and digested with RNase. The RNA-labeled proteins were precipitated at 4°C overnight with 20 µl protein A agarose (Santa Cruz Biotechnology) and 2.5 µg affinity purified antibodies or rabbit IgG in 1 ml 120 mM Tris-HCl pH 8.0, 120 mM NaCl, 1 mM EDTA, 0.5% NP40, 4% (v/v of stock solution) proteinase inhibitor cocktail Complete (Roche), washed thrice with 1 ml of the same buffer and eluted.

### **2.2.3 Cell Biology techniques**

#### **2.2.3.1 Preparation and transfection of primary hippocampal neurons**

Preparation and transfection of primary hippocampal neurons were basically performed as described (Blichenberg *et al.* 1999) with the following modifications. Neurons from the hippocampi of rat E18-E20 embryos were grown in MODIFIED EAGLE MEDIUM (MEM, Gibco) with 10% (v/v) horseserum (Gibco) for 3 hours at 37°C on poly-L-lysine (Sigma) coated coverslips washed with sterile water. The cells were further

grown in NEUROBASAL medium (NB, Gibco) supplemented with B27 (Gibco), 0.5 mM L-glutamine and 25 $\mu$ M glutamate. Four days later, half of the medium from each well was removed and fresh NB medium with 5  $\mu$ M AraC (Cytosine- $\beta$ -D-Arabinofluranoside, Sigma) was added to remove glial cells from culture.

Neurons were transfected with the calcium phosphate precipitation method on day 7 as follows. To 10  $\mu$ g plasmid DNA (endotoxin-free) and 10  $\mu$ l 2.5 mM CaCl<sub>2</sub> in a final volume of 100  $\mu$ l, 100  $\mu$ l 2x BBS (50 mM BES, 280 mM NaCl, 1.5 mM Na<sub>2</sub>HPO<sub>4</sub>, pH 6.96) was added drop-wise while continuously vortexing the reaction tube. The precipitate thus formed was incubated at RT for 20 min and 100  $\mu$ l of the mix was added to the medium of each well. The cells were placed back in the incubator and 3-4 hours after transfection, the fine precipitate formed was washed off from the cells by washing twice with 1x HBSS (10x HBSS; Gibco, 10mM HEPES, 2 mM NaOH). Fresh neurobasal medium was added to the cells.

### **2.2.3.2 Immunocytochemistry and *in situ* hybridization in primary neurons.**

Immunocytochemistry in primary neurons was carried out as follows. Neurons were fixed for 15 min at RT in 4% paraformaldehyde, 4% sucrose in PBS and permeabilized with 0.3% Triton-X-100 (Sigma) in PBS for 5 min at RT. Alternatively, cells were fixed in ice-cold methanol for 4 min at -20°C. Fixed cells were washed thrice with 4% sucrose in PBS, blocked for 30 min at room temperature in 10% normal goat serum (NGS, Gibco) in PBS, and incubated with the primary antibodies appropriately diluted in 10% NGS in PBS at 4°C overnight. The cells were washed thrice with PBS at RT for 5 min each, and incubated for 1 hour at RT with either Alexa<sub>488</sub>,

Alexa<sub>546</sub>, and Marina blue coupled secondary antibodies diluted in 10% NGS in PBS. The neurons were washed as before, equilibrated in water, air-dried and mounted on slides with Permafluor (Beckman Coulter).

For blocking experiments, affinity purified MARTA2 antisera N54, C98 and C99 were pre-incubated with MARTA2-GST fusion proteins (20 µg/mL) at 4°C overnight. Neurons fixed with methanol were incubated with the blocked antibodies followed by the normal immunocytochemistry method described above.

*In situ* hybridization, in neurons was performed following the procedure described in Blichenberg *et al.* (1999) with the following modifications. Following hybridization, the DIG-labeled probe was detected immunocytochemically by incubation with mouse monoclonal Cyanine-3 (Cy3)-coupled digoxigenin antibody in blocking buffer overnight at 4°C. For detection of EGFP fusion proteins in transfected neurons, rabbit GFP antibody was added to the diluted Cy3-coupled digoxigenin antibody. Cy3-coupled goat anti-mouse and Alexa<sub>488</sub>-coupled goat anti-rabbit secondary antibodies were used to fluorescently visualize the DIG-labeled RNA and EGFP proteins respectively. MAP2 was detected subsequently with polyclonal rabbit MAP2 antibody for 4 hours at RT or overnight at 4°C in blocking buffer followed by detection with Marina Blue-coupled goat-anti rabbit secondary antibody. Neurons were washed in buffer 1 and mounted as described above.

### **2.2.3.3 Detergent extraction for primary neurons**

Neurons were rinsed briefly with PBS and washed once with extraction buffer (100 mM Pipes, 1 mM MgSO<sub>4</sub>, 2 mM EGTA, 1.8 M glycerol). The cells were then treated with the same buffer containing 0.2% Triton-X-100 for 10 min at RT. Subsequently, the cells were washed carefully twice with

extraction buffer and fixed with ice-cold methanol as described in 2.2.3.2.

#### **2.2.3.4 Immunogold labeling in tissue sections**

For immunogold electron microscopy, animals were deeply anaesthetized by a mixture of ketanest and rompun and perfused through the heart with 4% paraformaldehyde and 0.1% glutaraldehyde in PBS. Sixty  $\mu\text{m}$  vibratome sections of the brain were cryoprotected in an ascending series of 0.5 M, 1 M, 1.5M and 2 M sucrose and subjected to two freeze-thaw cycles in liquid nitrogen to aid penetration of immunoreagents. Sections were blocked for 1 hour in 10% NGS and 0.2% BSA (bovine serum albumin) in PBS at room temperature and incubated with purified MARTA2 antiserum diluted to the working concentration in 1% NGS and 0.2% BSA in PBS at 4°C overnight. The sections were then incubated with a goat-anti rabbit coupled to nanogold (Nanoprobes) in 1:100 dilution for 2 hours at RT. Labeling was subsequently followed by gold toning with 0.05% gold chloride (Sigma) in 150 mM sodium acetate buffer. After fixation with 1% osmiumtetroxide, cultures were dehydrated in an ascending series of ethanol and embedded in Epon (Roth). The ultrathin sections were examined with Zeiss EM 902 microscope.

#### **2.2.3.5 Microscopy and quantification.**

Visualization and documentation of the fluorescence signals were done with either a Zeiss Axiovert 135 microscope in combination with a CCD C4742-95-12NRB digital camera (Hamamatsu) and the OpenLab 2.2.5 software (Improvision), or a confocal laser-scanning microscope (Leitz). Images were mounted using Adobe Photoshop CS software (Adobe Systems Incorporated). Counting of MAP2 mRNA granules in dendrites was done using the line measurement tool provided in the

OpenLab software. With the help of a graticule, images were calibrated such that 10  $\mu\text{m}$  length is equal to 66 image pixels. 60  $\mu\text{m}$  of proximal dendrite length was measured per neuron and the individual RNA granules were counted within the measured length. Graphical representation was done using the Excel program (Microsoft).

## **CHAPTER 3: RESULTS**

### **3.1 Dendritic distribution of MAP2 mRNA in cultured neurons.**

#### **3.1.1 Targeting of MAP2 mRNAs into dendrites is an early event during neuronal differentiation.**

In neurons, selective mRNAs are targeted to dendrites where their translation is modulated by neuronal activity. MAP2 mRNA transcripts were the first mRNAs to be identified in somata and in dendrites of neurons in the rat brain (Garner *et al.* 1988). Subsequently, using radioactively labeled probes it was shown that this subcellular distribution pattern of MAP2 mRNAs is preserved in cultured primary neurons derived from rat superior cervical ganglia (SCG) and the hippocampus (Bruckenstein *et al.* 1990; Kleiman *et al.* 1990). The radioactive signal representing MAP2 mRNA were granular in the somata and in dendrites of both hippocampal and SCG neurons in culture (Bruckenstein *et al.* 1990). In contrast, the distribution pattern of  $\beta$ -tubulin mRNA was restricted to the somata in both types of neuronal cultures (Brukenstein *et al.* 1990; Kleiman *et al.*, 1990). To study the nature and distribution of MAP2 transcripts with a spatial resolution relatively higher than the radioactive signals, endogenous MAP2 mRNA was visualized in cultured hippocampal neurons by fluorescence *in situ* hybridization (FISH). While no significant signal was detected with the sense riboprobe (figure 4,C), hybridization with the anti-sense riboprobe resulted in a strong signal that was present in both somata and in neuronal processes (figure 4,A). Despite of the fact that hippocampal neurons in culture also contain a low fraction of glial cells and fibroblasts (Banker and Goslin 1988), the signal for MAP2 mRNA was only seen in cells that were

immunopositive for MAP2, a neuronal marker protein (Caceres *et al.* 1984; Caceres *et al.* 1984) (figure 4,B & D). Moreover, MAP2 RNA was not evenly distributed throughout the somatodendritic cytoplasm but resided in distinct granules that were visible in somata and along dendritic shafts (see enlarged images, arrowheads). Typically, mRNAs are localized in the form of RNP particles to their target sites (Kindler *et al.* 2005). The size of the individual granules implies that MAP2 mRNA molecules are components of large macromolecular complexes or RNP particles that may represent transport units and/or anchoring sites. In contrast to MAP2 mRNA distribution, visualization of  $\beta$ -tubulin mRNA via *in situ* hybridization revealed that the mRNA was present only in the somata (figure 4, E and F). No signal was detected with the  $\beta$ -tubulin sense riboprobe. Hence, in neurons only a selected group of mRNAs is localized to dendrites while others remain restricted to the somata.

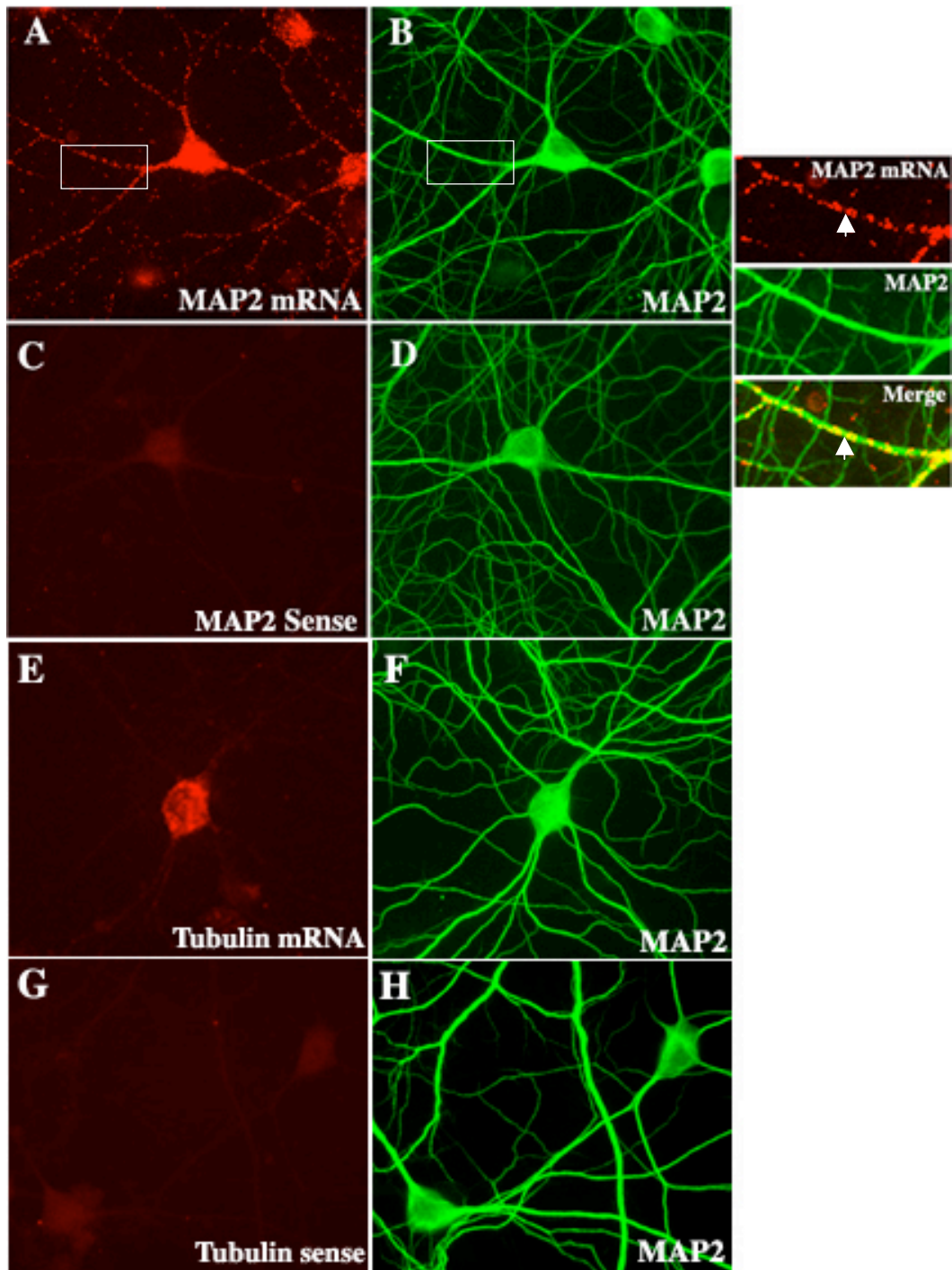


**FIGURE 4**

**Distribution of MAP2 mRNA and  $\beta$ -tubulin mRNA visualized in primary hippocampal neurons by FISH analysis.** Hybridization with a digoxigenin (DIG)-labeled riboprobe complementary to the coding region of the MAP2 sequence (anti-sense) resulted in a somatodendritic signal (A). In contrast, the sense probe gave no signal upon hybridization (C). Similarly, the sense probe for  $\beta$ -tubulin resulted in no signal (G) whereas the anti-sense probe showed that  $\beta$ -tubulin mRNA is restricted to the somata (E). Following hybridization, the DIG-labeled probes were detected with a Cy3-coupled mouse digoxigenin antibody (red) and an anti-mouse IgG-Cy3-coupled antibody from goat (red). MAP2 protein was detected in parallel as a dendrite marker (B, D, F, and G) using a rabbit polyclonal MAP2 antiserum and Alexa<sub>488</sub>-coupled secondary goat antibody (green). MAP2 mRNA was seen as granules along MAP2 positive dendrites (see enlarged side images and arrowheads) in contrast to  $\beta$ -tubulin mRNA, which were seen only in the somata. Scale bars: 25  $\mu$ m.

The difference in the distribution pattern of MAP2 and  $\beta$ -tubulin mRNAs demonstrates that a selected number of mRNAs are somatodendritically localized in neurons. *In situ* hybridization studies have indeed shown that very few mRNA transcripts are present in dendrites (Eberwine *et al.* 2002). Yet, it is unclear as to when during neuronal differentiation, dendritic mRNA targeting first takes place. The establishment of FISH analysis as a method to visualize MAP2 mRNA served as a tool to investigate the developmental time frame in which MAP2 transcripts are targeted into dendrites. For this purpose, I fixed cultured hippocampal neurons at 1, 3, 5, 7, and 14 days in vitro (div). During early developmental stages, neuronal processes may not be clearly defined as axons or dendrites and are hence, collectively referred as “neurites” (Goslin and Banker 1989; Goslin *et al.* 1990). Results from two independent experiments reveal that in neurons from all investigated developmental stages, MAP2 mRNA granules are visible along the entire length of neurites, which appear to be MAP2-positive (figure 5, P1-P14), and, are more or less evenly distributed. The above experiment demonstrates that MAP2 mRNA is dendritically localized at a very early developmental time point.

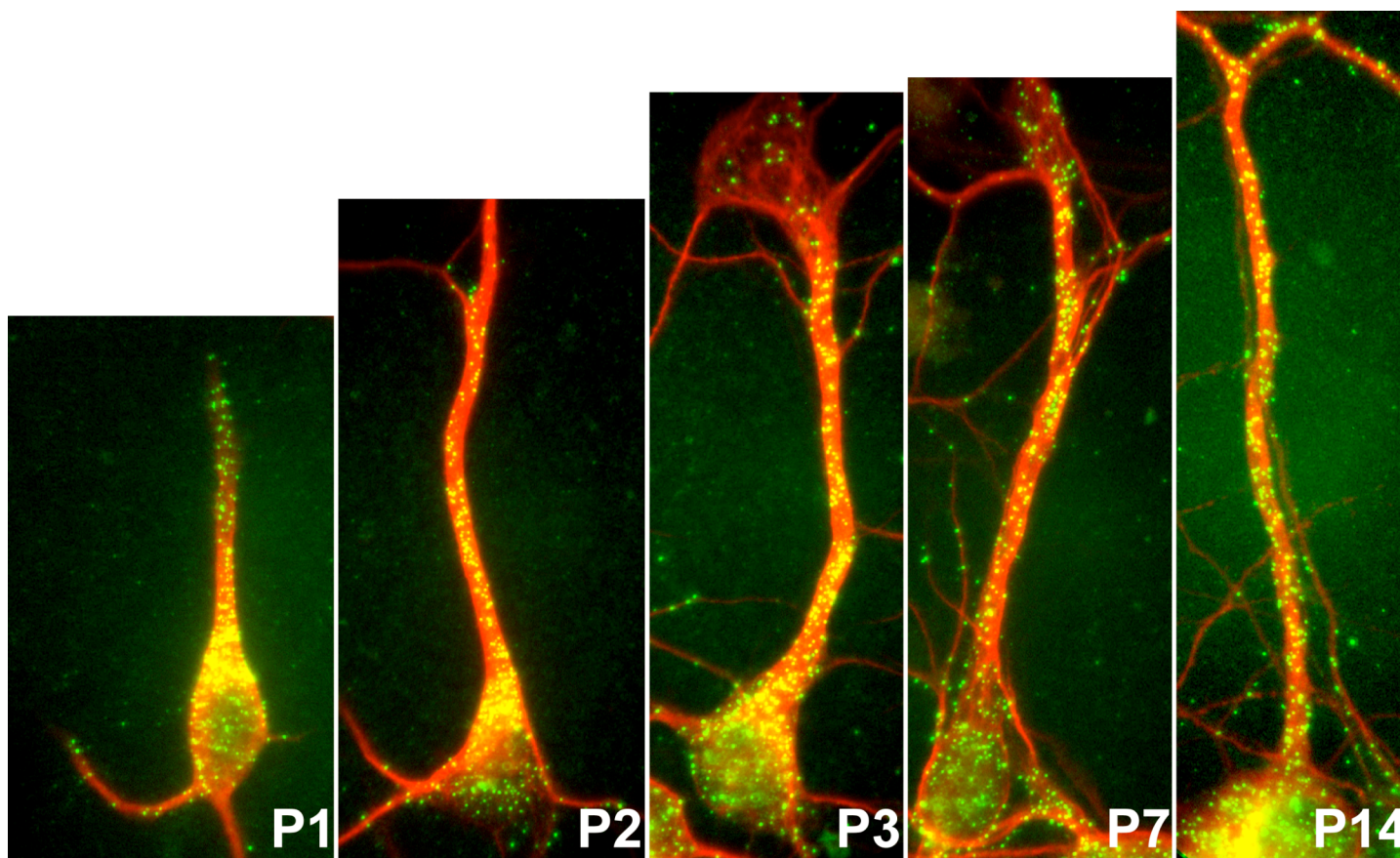


**FIGURE 5**

**MAP2 mRNA targeting to neurites of primary hippocampal neurons is an early event during neurogenesis in culture.** The hybridized dig-labeled MAP2 anti-sense riboprobe was originally detected with a mouse Cy3-coupled dig. antibody (red) and a Cy3-coupled secondary antibody from goat (red). MAP2 protein was actually visualized using a rabbit polyclonal antiserum against MAP2 and Alexa<sub>488</sub>-coupled secondary goat antibody (green). However, for better visibility of MAP2 mRNA granules along the MAP2-positive neurites in the merged images, MAP2-positive neurites are shown here in red while MAP2 mRNA granules are depicted in green. Primary neurons were fixed after 1, 2, 3, 7 and 14 days in culture (P1-P14). The mRNA granules were more or less evenly distributed along the entire length of the main neurite that is MAP2-positive and therefore, appear as yellow in the merged images.

## **3.2 Characterization of the MAP2 mRNA trans-acting factor MARTA2.**

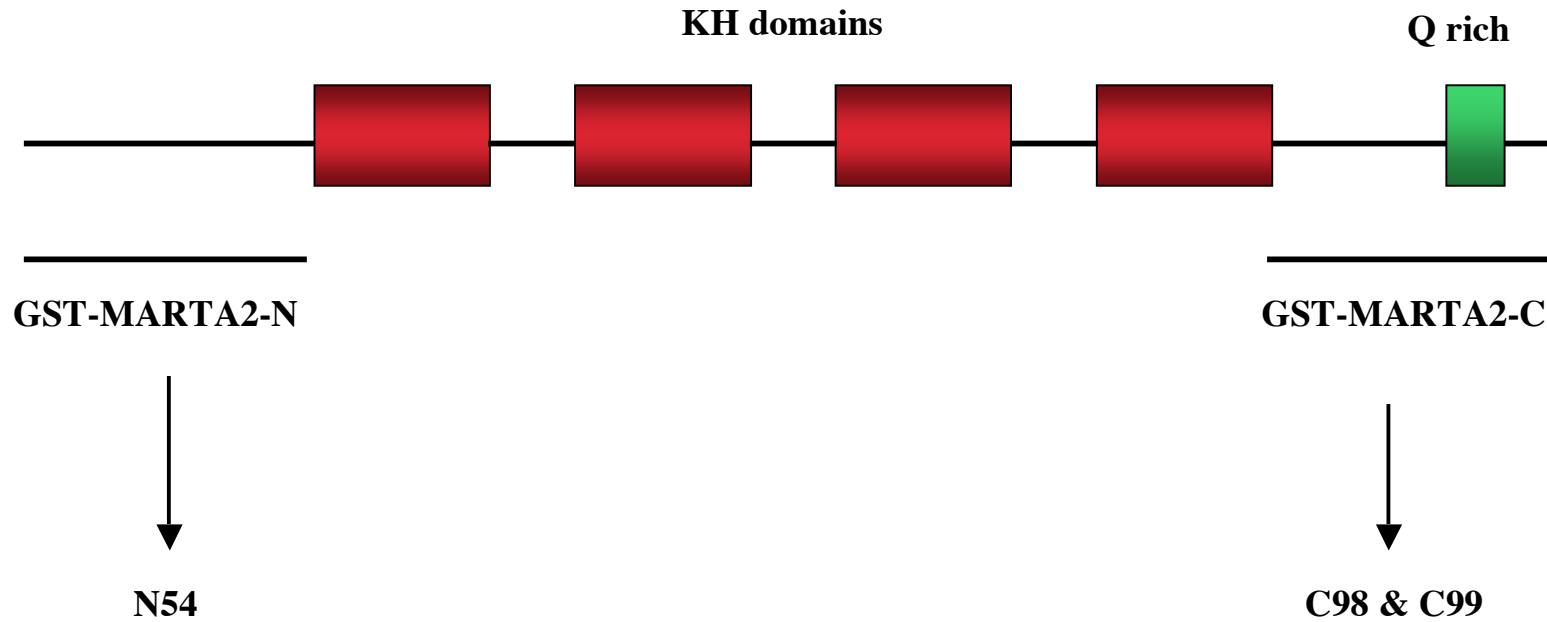
### **3.2.1 Generation of antibodies against MARTA2.**

mRNA transport involves the recognition of a *cis*-acting targeting element present within localized mRNAs by *trans*-acting RNA-binding proteins (Kindler *et al.*, 2005). A 640 nucleotide spanning *cis*-acting DTE in the 3'UTR of MAP2 transcripts mediates extrasomatic localization (Blichenberg *et al.* 1999). Two *trans*-acting factors namely MARTA1 and MARTA2 specifically interact with the MAP2-DTE (Rehbein *et al.* 2000). MARTA2 was recently purified from the rat brain and mass spectrometric analysis revealed that the protein is the rat ortholog of FBP3 (Zivraj *et al.* in preparation). The prototypical member of the FBP family namely FBP1 is shown to bind to the FUSE element of the *c-myc* oncogene and is involved in its transcriptional regulation (Duncan *et al.* 1994). Typical of the members of the FBP family, MARTA2 contains four central KH domains that bind single-stranded DNA/RNA (figure 6).

For the generation of antibodies, two different parts of the MARTA2 cDNA coding region (GenBank accession number DQ144645, nucleotides 1-310 and 1270-1710, respectively) were sub-cloned into the vector pGEX-6P-3 and expressed in bacterial cells. Corresponding glutathione S-transferase (GST) fusion proteins (N-MARTA2-GST and C-MARTA2-GST) were affinity purified from bacterial lysates. Three different polyclonal antisera (N54, C98, and C99) were thus raised in rabbits against the N- or the C-terminal parts of MARTA2 and affinity purified. To test their specificity, all three MARTA2 antisera were used to immunoprecipitate proteins from a UV cross-linking assay performed with RSW proteins and a radioactively labeled MAP2-

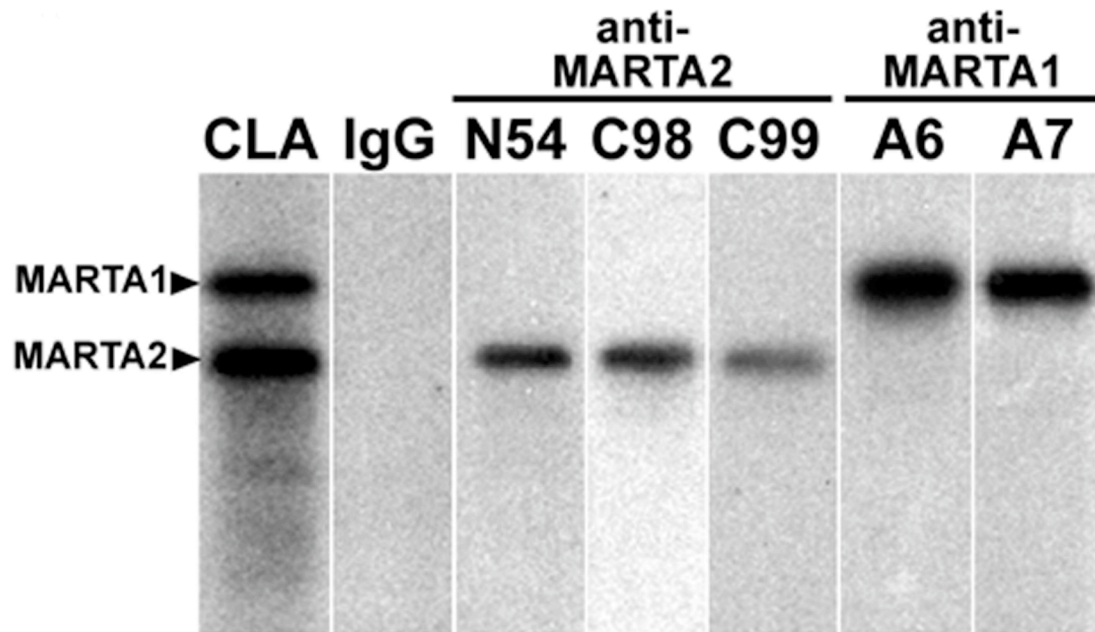
DTE probe (figure 7, CLA). All three antibodies specifically precipitated the 65 kDa cross-linked MARTA2 (figure 7, N54, C98, and C99), whereas DTE-linked MARTA1 remained in the supernatant fraction. Conversely, only the 90 kDa RNA-bound MARTA1 but not MARTA2 was precipitated with two different MARTA1-specific antibodies (figure 7, A6 and A7). Neither MARTA2 nor MARTA1 were precipitated with unspecific IgGs (figure 7, IgG). These findings confirm that MARTA2 indeed represents the 65 kDa MAP2-DTE binding protein observed in UV cross-linking assays (figure 7, CLA and Rehbein *et al.* 2000). In addition, all three MARTA2 antisera do not cross-react with MARTA1.

## Domain structure of MARTA2



**FIGURE 6**

**Generation of MARTA2 antisera.** The schematic representation of MARTA2 shows that it contains four central KH domains (red boxes) that bind to single-strand DNA /RNA. The C terminal part of the protein has a 146 amino acid residue long stretch containing 48% glutamate residues (green box). GST fusion proteins, GST-MARTA2-N and GST-MARTA2-C were generated and injected in rabbits to raise antisera against N- and C-terminal domains of MARTA2 namely N54 C98 and C99.

**FIGURE 7**

**Immunoprecipitation of cross-linked MARTA proteins.** Autoradiograph of UV cross-linked proteins separated on a SDS-polyacrylamide gel. For each immunoprecipitation, 10  $\mu$ g protein from a RSW fraction of adult rat brain were incubated with 20 fmoles of MAP2-DTE probe, cross-linked with UV and digested with RNase. The RNA probe is cross-linked to the 65 kDa and 90 kDa proteins, MARTA2 and MARTA1 (CLA). Immunoprecipitation performed with either MARTA2 (N54, C98, and C99) or MARTA1 (A6 and A7) specific antibodies, selectively contain the respective RNA-labeled proteins. Immunoprecipitation with unspecific IgGs is devoid of both proteins (IgG).

### **3.2.2 Subcellular distribution of MARTA2 in the adult rat brain.**

To investigate the subcellular distribution of MARTA2, I performed Western blotting using different rat brain fractions and the polyclonal antiserum N54. While MARTA2 was barely detectable in the crude lysate and the cytosolic fraction (figure 8A, lanes 2 and 3, respectively) it was clearly present in the nuclear (figure 8, lane 1) and the polysome fractions (figure 8, lane 4). A strong enrichment of MARTA2 was seen in the RSW fraction (figure 8, lane 5). Polyclonal antisera C98 and C99 essentially gave identical results on a Western blot (data not shown). Antisera specificity was confirmed by preincubating the antisera with GST-MARTA2 fusion proteins. The N54 antiserum was preincubated with N-GST-MARTA2 while the C98 and the C99 antisera were preincubated with C-GST-MARTA2 fusion protein. All three blocked antisera failed to recognize MARTA2 in the polysome fraction by Western blot analysis (figure 8B). The fact that MARTA2 is hardly detectable in the crude lysate, suggests that the overall amount of the protein present in the brain is low. This was verified by immunoprecipitation of the protein from crude lysate with the C98 antiserum (figure 8C, lane 1). Western blot analysis of the immunoprecipitated material using the N54 antiserum showed that MARTA2 could be immunoprecipitated from crude lysate (figure 8,C, lane 1) in contrast to the immunoprecipitation performed with unspecific rabbit IgGs (figure 8C, lane 2). Hence, the above results indicate that low amounts of MARTA2 are present in the rat brain where it is mainly associated with polysomes and is also present in the nucleus.

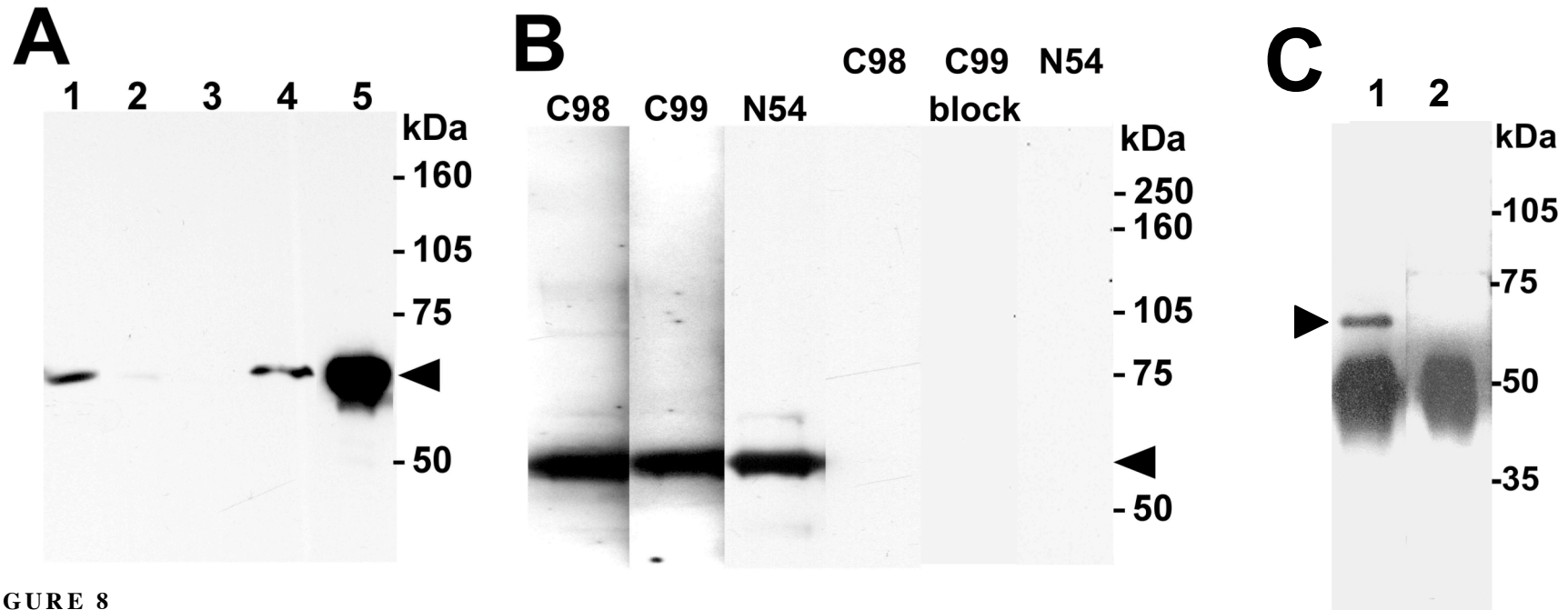


**FIGURE 8**

**Subcellular distribution of MARTA2 in the rat brain.** (A) Western blot performed with affinity purified N54 antiserum and 40  $\mu$ g protein each from different rat brain fractions (nuclear fraction, crude lysate, S100 cytosolic fraction and polysome fraction; lanes 1- 4 respectively) and 20  $\mu$ g RSW protein (lane 5). The antiserum specifically detects the 65 kDa MARTA2 that is strongly enriched in the RSW (note that only half of the protein amount is loaded in lane 5 containing proteins from the RSW). (B) Western blot performed with affinity-purified C98, C99 and N54, which were raised against C- and N-terminal parts of MARTA2, and 40  $\mu$ g protein from a rat brain polysome fraction. All antisera recognize MARTA2 at 65 kDa. Preincubation of the antisera with the corresponding N-MARTA2-GST and C-MARTA2-GST fusion proteins abolish MARTA2 detection in the polysome fractions. (C) Immunoprecipitation of MARTA2 from 1 mg rat brain crude lysate using C98 antisera. The protein is immunoprecipitated as visualized in Western blot using N54 antiserum (lane 1). In contrast, the protein was not detected when unspecific rabbit IgGs were used for immunoprecipitation instead of the C98 antiserum.

### **3.2.3 MARTA2 distribution in cultured hippocampal neurons.**

MARTA2 distribution in two weeks old primary hippocampal neurons was studied by immunocytochemistry using MARTA2 specific antisera described in 3.2.1 and 3.2.2. MARTA2 antiserum N54 for instance, detected the protein predominantly in the somatodendritic compartment of the cell although it was also seen in the nucleus. Figure 9 shows images of MARTA2 in primary neurons having a granular distribution along MAP2 positive dendritic shafts (see insets in A and B). Analogous to the Western blot results (figure 8B), pre-incubation of the N54 antiserum with N-GST-MARTA2 fusion protein abolished MARTA2 immunoreactivity in primary neurons (figure 9C). Similar results were obtained with both antisera directed against the C-terminus (C98 and C99). Immunocytochemistry with C98 and C99 revealed a somatodendritic distribution of MARTA2 as granules along dendritic shafts. Both sera after pre-incubation with C-GST-MARTA2 fusion protein failed to immunoreact with the MARTA2 antigen in neurons (data not shown).

It is to be noted here that the subcellular distribution pattern of MARTA2 as determined by immunocytochemistry, partially depends on the fixative that is used to fix the cells. In neurons fixed with ice-cold methanol, MARTA2 exhibited the granular somatodendritic pattern as described above (figure 10, B). However, in cells that were fixed with 4% paraformaldehyde (PFA) and 4% Sucrose in PBS, followed by permeabilization with 0.3% Triton-X-100 in PBS, MARTA2 immunostaining in the somatodendritic cytoplasm was weaker and considerably more diffuse (figure 10, A). Nevertheless, the granular distribution pattern of endogenous MARTA2 in primary neurons indicates that the protein is present in RNP particles.

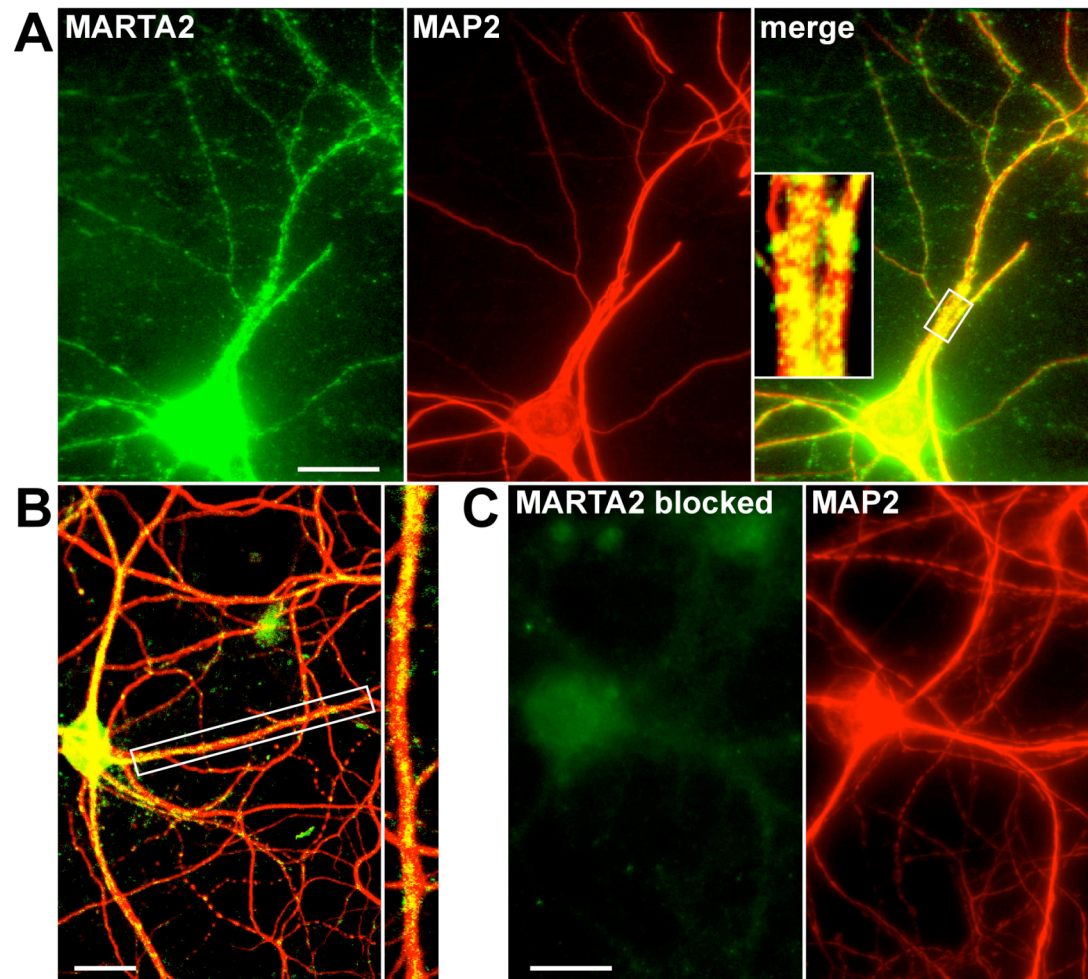


**FIGURE 9**

**MARTA2 distribution in primary hippocampal neurons.** Two weeks old cultured hippocampal neurons (A and B) were immunostained with polyclonal MARTA2 antiserum N54 and a monoclonal antibody against endogenous MAP2. MARTA2 (green) is present in the MAP2-positive (red) somatodendritic cytoplasm of primary neurons (A and B). Insets in the merged pictures shown in panels A and B are enlargements of boxed dendritic regions to better visualize MARTA2 granules (yellow) distributed along MAP2-positive dendritic shafts. (C) When the MARTA2 antiserum N54 is preincubated with recombinant N-MARTA2-GST antigen, the respective immunochemical signal on primary neurons is entirely lost (left panel), whereas endogenous MAP2 is still detected in the cell (right panel). MARTA2 and MAP2 are visualized with Alexa<sub>546</sub>- and Alexa<sub>488</sub>-coupled secondary goat antibodies, respectively. Micrographs from panel A and C were captured with a conventional fluorescence microscope, whereas the merged image shown in panel B represents a 0.5  $\mu\text{m}$  optical section of a primary neuron that was taken with a laser-scanning microscope. Distinct MARTA2 granules along dendritic shafts are more apparent in the laser-scanning micrograph. Scale bars: 25  $\mu\text{m}$ .

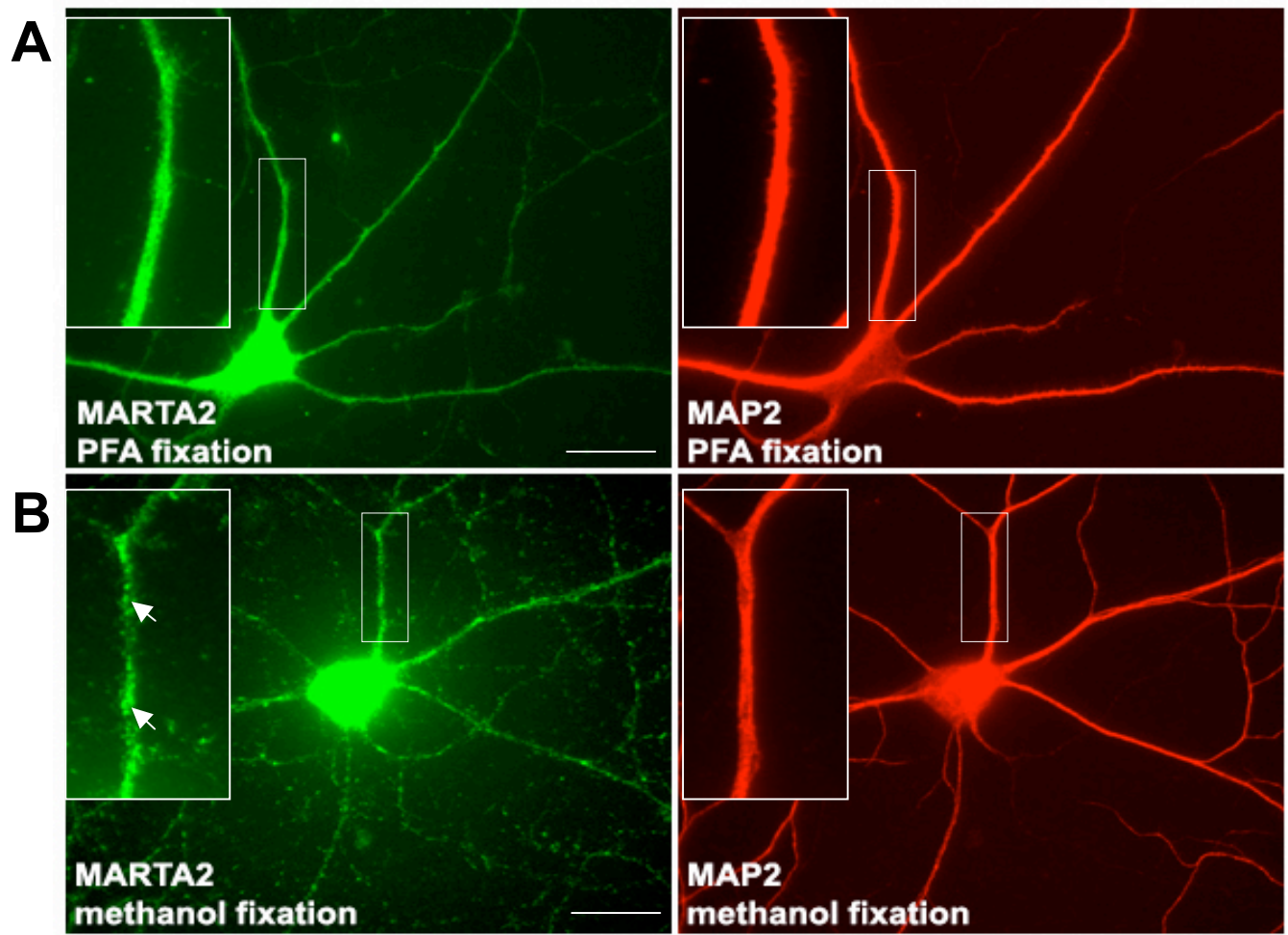


**FIGURE 10**

**MARTA2 immunodetection in primary neurons depends on the fixative agent.** (A) In neurons fixed with 4% PFA and 4% sucrose in PBS, and permeabilized with 0.3% Triton-X-100 in PBS, immunodetection of MARTA2 with polyclonal N54 antiserum shows considerably weak and diffuse somatodendritic distribution of the protein (see inset) (B) In contrast, in methanol fixed neurons, MARTA2 is seen as distinct granules along dendritic shafts (inset and arrows). MAP2 was detected in parallel with a mouse antibody against MAP2 and Alexa<sub>488</sub>-coupled secondary goat antibody (green). The two proteins were detected as described in figure 9. Scale bars: 25 µm.

#### **3.2.4 MARTA2 fusion proteins mimic endogenous MARTA2 distribution in neurons.**

The influence of the fixative agent gave conflicting results on the distribution of endogenous MARTA2 in neurons. Hence, MARTA2 fusion proteins were transiently expressed in neurons to give further insight into the distribution pattern of the protein. The coding region of MARTA2 cDNA (accession number DQ144645, nt 1-1710) was cloned into eukaryotic expression vectors such that the encoded protein is tagged either at its N- or at its C-terminus. One-week old neurons expressing either recombinant EYFP-MARTA2 or MARTA2-EGFP were fixed with 4% PFA and 4% sucrose in PBS, permeabilized with 0.3% Triton-X-100 in PBS, and immunostained for MAP2 protein. The fusion proteins were directly visualized by their auto-fluorescence. Both recombinant proteins irrespective of the relative position of the tag were seen in dendrites as distinct granules in neurons (figure 11 A and C, see enlarged images, arrows). The above data confirm that MARTA2 is indeed distributed as granules in hippocampal neurons underlining the possibility of its presence in RNP particles.

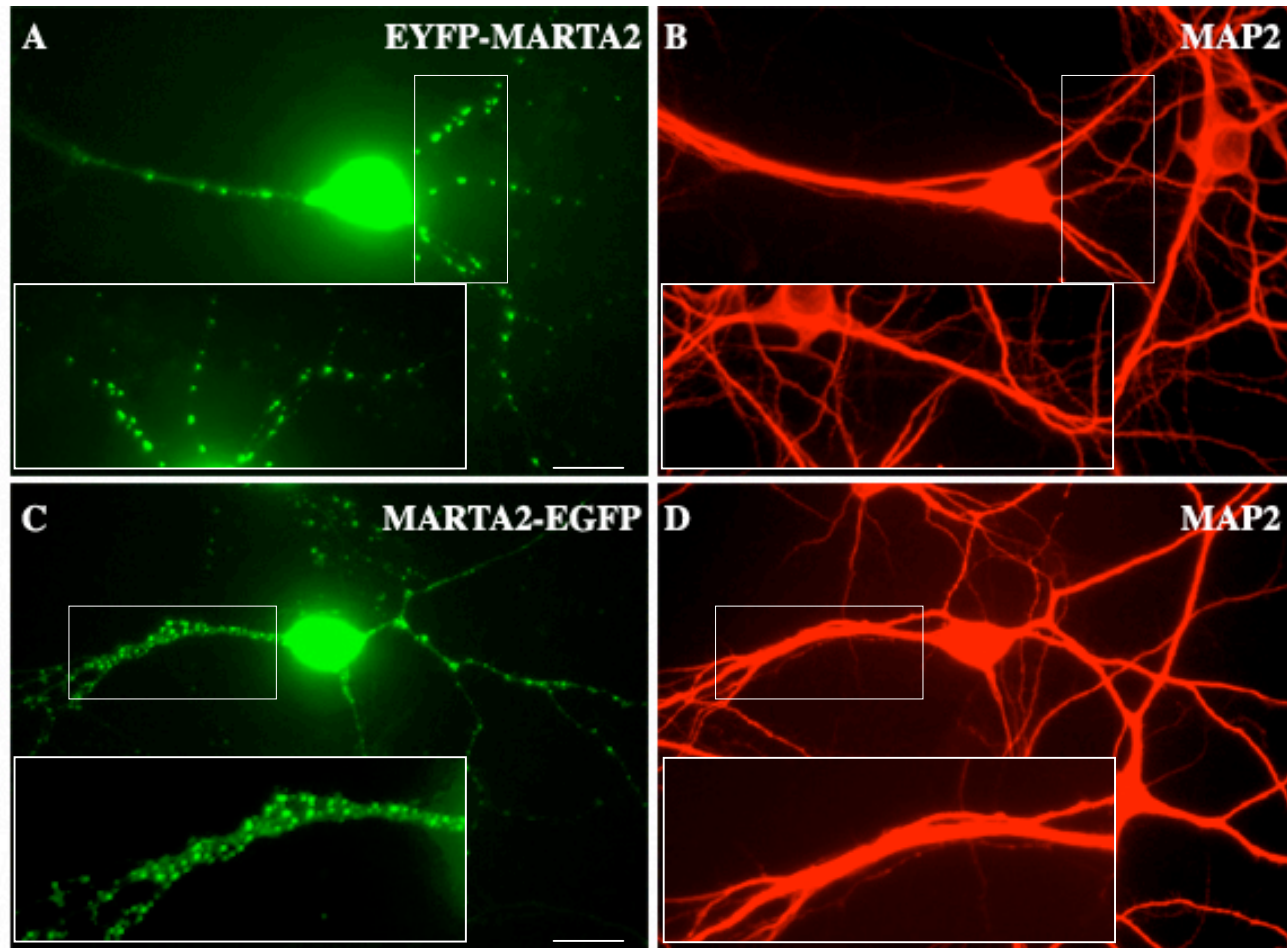


**FIGURE 11**

**MARTA2 fusion proteins mimic the endogenous protein in their neuronal distribution.** Recombinant MARTA2 fused to an EYFP-tag at the N-terminus (A) or to an EGFP-tag at the C-terminus (C) was detected in hippocampal neurons in the form of discrete granules. Immunostaining for endogenous MAP2 served as a dendrite marker (B and D). While the recombinant proteins were visualized by their auto-fluorescence, mouse antibody against MAP2 and Alexa<sub>546</sub>-coupled goat secondary antibody were used to detect MAP2.

### **3.2.5 MARTA2 is associated with the cytoskeleton.**

In different cell systems, RNA transport involves cytoskeletal components such as microtubules and microfilaments (Kindler *et al.* 2005). The granular distribution of MARTA2, which suggests its presence in RNP particles served as a propeller to study its association, if any, with the neuronal cytoskeleton. Two weeks old primary hippocampal neurons were treated with a detergent-containing buffer prior to methanol fixation. Under these conditions, all soluble cytosolic components of the cell are released whereas the cytoskeleton remains intact. In non-treated cells, MARTA2 and MAP2 (figure 12 A and B) were detected in the somatodendritic compartment. Glyceraldehyde-3-phosphate dehydrogenase (GAPDH), a soluble protein was also found in somata and along dendrites (figure 12 C). However, in detergent-treated neurons, most of GAPDH that is known to be a soluble component of the cytoplasm was extracted from the cells (figure 12 E), while microtubule-associated MAP2 remained bound to the cytoskeleton of the same neurons (figure 12 B and F). Similarly, MARTA2 was also strongly detected in somata and in dendrites of neurons treated with detergent (figure 12 A). Furthermore, the protein was seen in the form of discrete granules (figure 12 A, inset and arrows). Hence, in hippocampal neurons, a majority of MARTA2 resides in granules that are associated with the somatodendritic cytoskeleton.

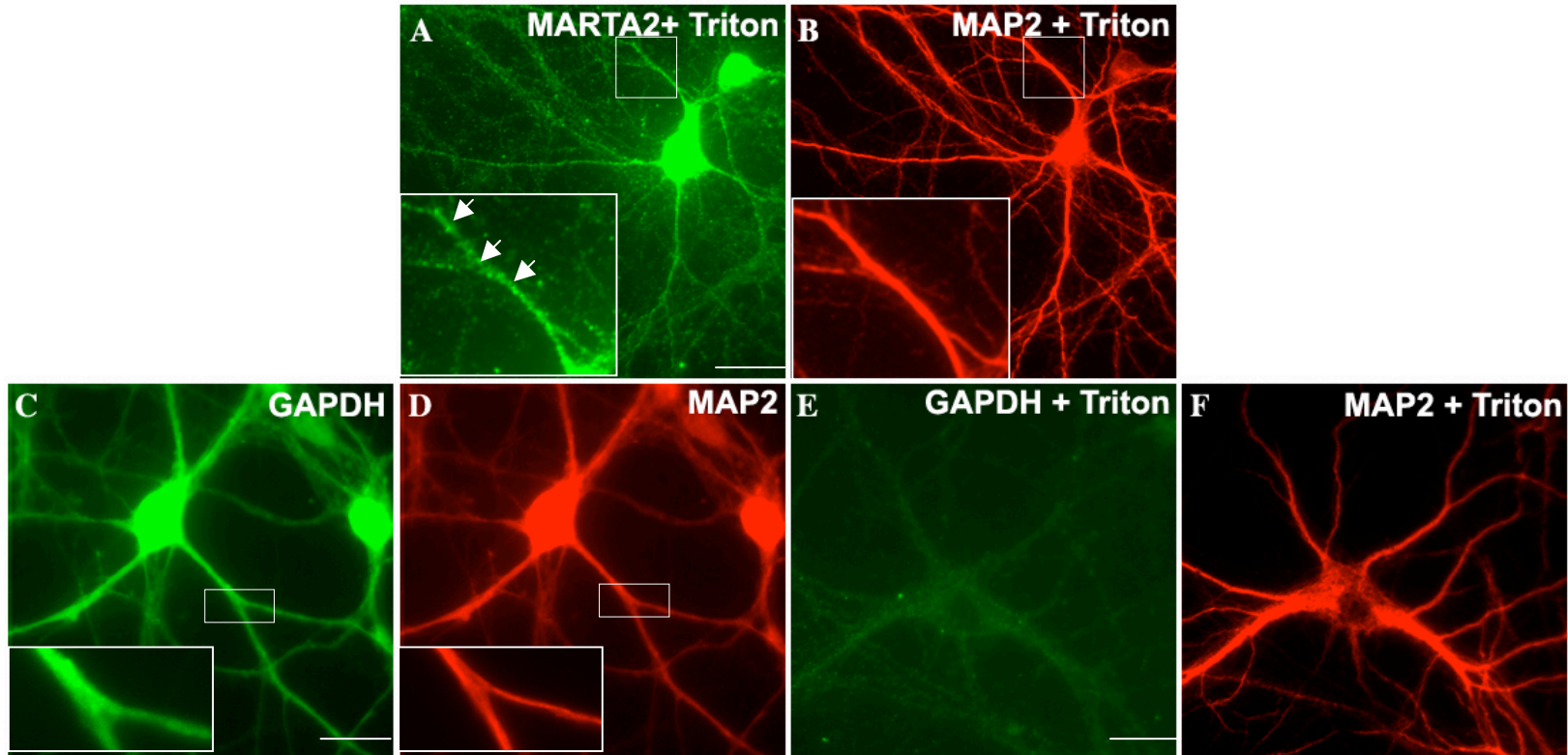


**FIGURE 12**

**Cytoskeletal association of MARTA2 in hippocampal neurons.** Immunocytochemistry was performed on two weeks old primary hippocampal neurons that were extracted with Triton-X-100 detergent containing buffer. In Triton-X-100 treated neurons, MARTA2 (in green) and MAP2 (in red) remained associated with the remaining cytoskeleton (A and B, respectively). On the other hand, soluble GAPDH which was homogenously distributed throughout the cytoplasm of non-treated cells (C, in green) was released almost completely from the cytosol following treatment (E). MAP2 was detected in parallel with GAPDH in both treated and non-treated cells (D and F, in red). Primary antibodies used were MARTA2 N54 antiserum, mouse MAP2 antibody and mouse GAPDH antibody for the corresponding antigens. The proteins were visualized with Alexa<sub>488</sub>- and Alexa<sub>546</sub>-coupled secondary goat antibodies. Scale bars: 25 μm.

### **3.2.6 MARTA2 resides in somata and dendrites of rat brain neurons.**

Immunocytochemical data obtained for the endogenous as well as recombinant MARTA2 in cultured primary hippocampal neurons gave insight into the protein's distribution as granules that are associated with the cytoskeleton. In addition to the above data obtained in cultured neurons, further analysis of the protein's distribution was done in adult rat brain sections. Immuno-gold electron microscopy (EM) confirmed the somatodendritic distribution of MARTA2 in neocortical pyramidal cells (figure 13 A and B). As opposed to cultured neurons, occasional postsynaptic localization of MARTA2 in dendritic spines of excitatory synapses was also observed via this method (figure 13 C).

Taken together, extensive studies on MARTA2's distribution in primary neurons and the rat brain using both biochemical and immunochemical methods strongly indicate that the protein localizes to the somatodendritic compartment of neurons most likely as RNP complexes that translocate along the cytoskeleton. These data paved way for elucidating the role of MARTA2 as a *trans*-acting factor for dendritic MAP2 mRNA localization.

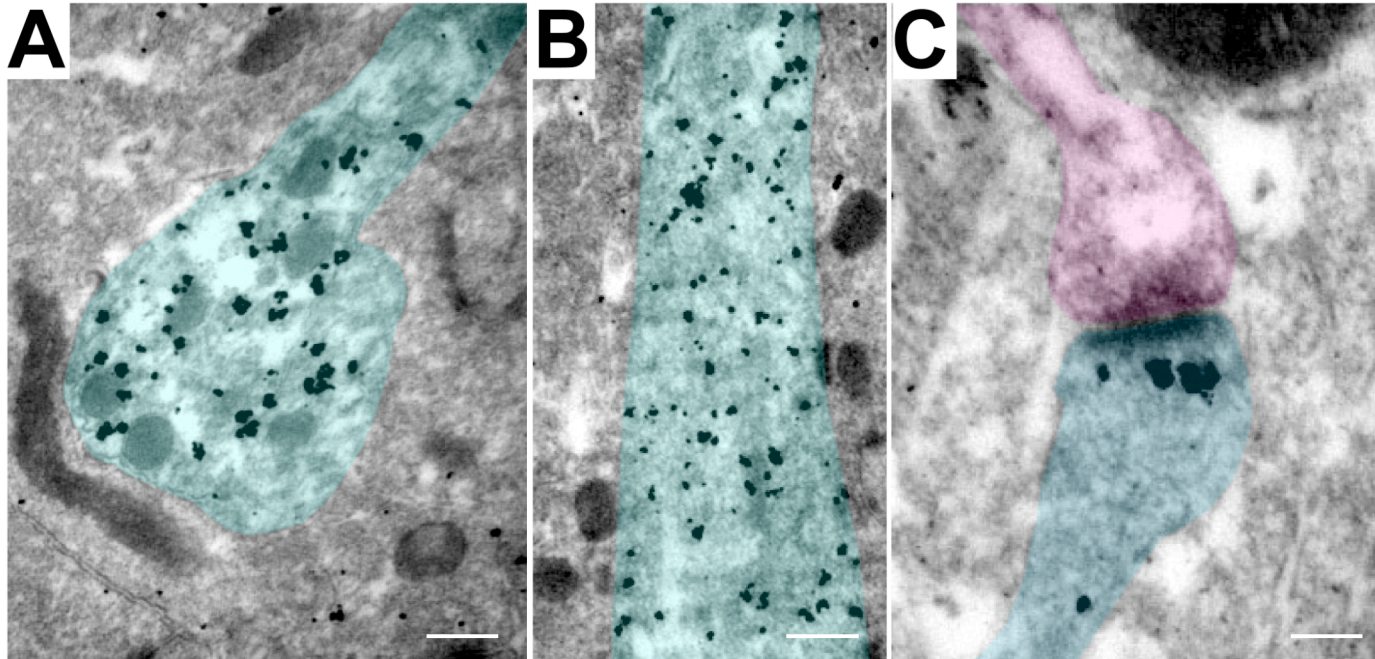


**FIGURE 13**

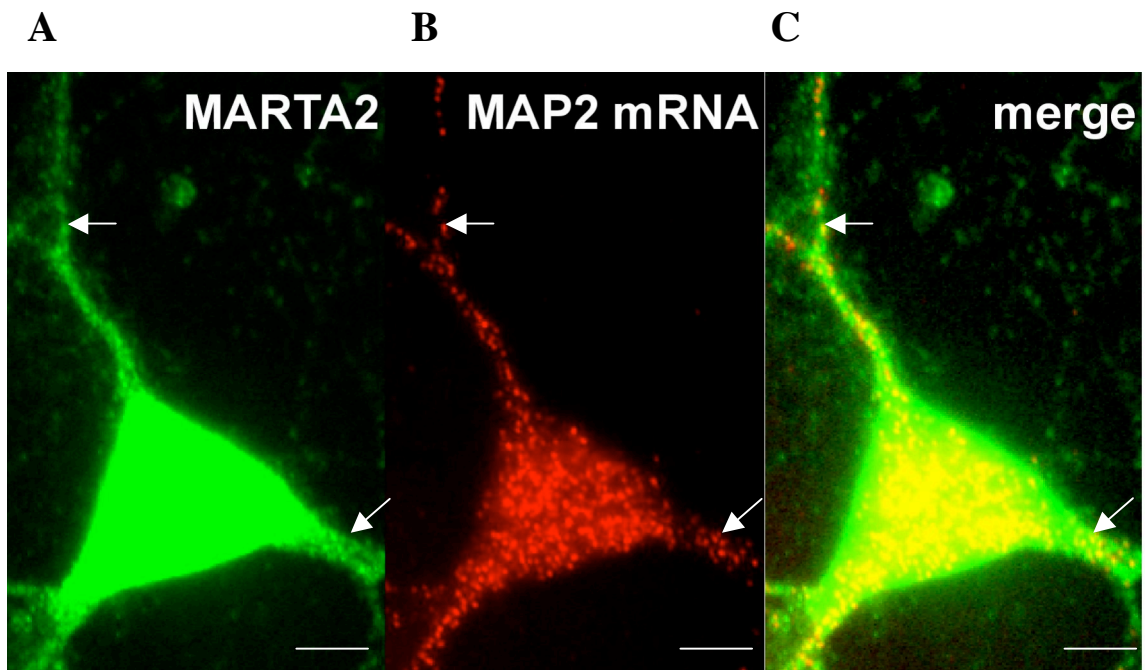
**Distribution of MARTA2 in adult rat brain neurons.** Coronal brain sections were immunostained with the polyclonal MARTA2 antiserum N54. In immunogold electron micrographs of the adult rat neocortex, gold particles representing the distribution of MARTA2 are seen in neuronal somata (A, highlighted in light blue; cell body is sectioned tangentially to the nucleus), along dendritic shafts (B, light blue), and in postsynaptic structures of excitatory synapses (C, light blue; presynaptic bouton is highlighted in pink). Panels A-C are bright light micrographs. Scale bars: 25  $\mu\text{m}$ .

### **3.3 Functional characterization of MARTA2.**

#### **3.3.1 Endogenous and recombinant MARTA2 co-localize with endogenous MAP2 mRNA *in situ*.**

Previous *in vitro* data show that MARTA2 specifically interacts with the MAP2-DTE (data presented herein, Rehbein *et al.* 2000). If MARTA2 also binds to MAP2 mRNA *in vivo*, both molecules should at least partially co-localize in neurons. To test the above hypothesis, simultaneous detection of MAP2 mRNA and MARTA2 protein was performed in cultured hippocampal neurons. However, as the RNA is washed out in methanol fixed neurons, neurons fixed with 4% paraformaldehyde were used for the study. As already mentioned in section 3.2.3, overall MARTA2 staining is reduced and distinct granules are not effectively detected under these conditions (figure 10 A). Hence, although MAP2 transcripts could be seen nicely as granules, MARTA2 staining is relatively weak and diffuse along dendrites. Superimposing images of MAP2 mRNA with MARTA2 revealed that MAP2 mRNA granules contained MARTA2 (figure 14). Yet, MARTA2 is also present at subcellular sites that do not contain MAP2 transcripts. This may hint towards an *in vivo* association of the RNA-binding protein with other neuronal mRNAs.

To overcome the technical limitation mentioned above, MARTA2-EGFP was expressed in primary neurons and endogenous MAP2 mRNA was visualized in neurons expressing MARTA2-EGFP. The recombinant protein (figure 15 A) showed a greater extent of co-localization with endogenous MAP2 mRNA transcripts (figure 15 B) in granules along dendritic shafts (figure 15, C). The above experiments accentuate the point that MARTA2 and MAP2 mRNA co-localize in granules in dendrites of primary neurons.

**FIGURE 14**

**Co-localization of endogenous MARTA2 with MAP2 mRNA in primary neurons.** In two weeks old hippocampal neurons, endogenous MARTA2 (A, polyclonal rabbit antiserum N54 and Alexa<sub>488</sub>-coupled goat secondary antibody) and MAP2 mRNAs (B, Cy3-coupled mouse digoxigenin antibody and Cy3-coupled goat secondary antibody) were visualized in a combined immunocytochemical and *in situ* hybridization assay. MARTA2 and MAP2 mRNAs partially co-localize in granular structures distributed along dendrites (C; arrows). Scale bars: 25  $\mu$ m.

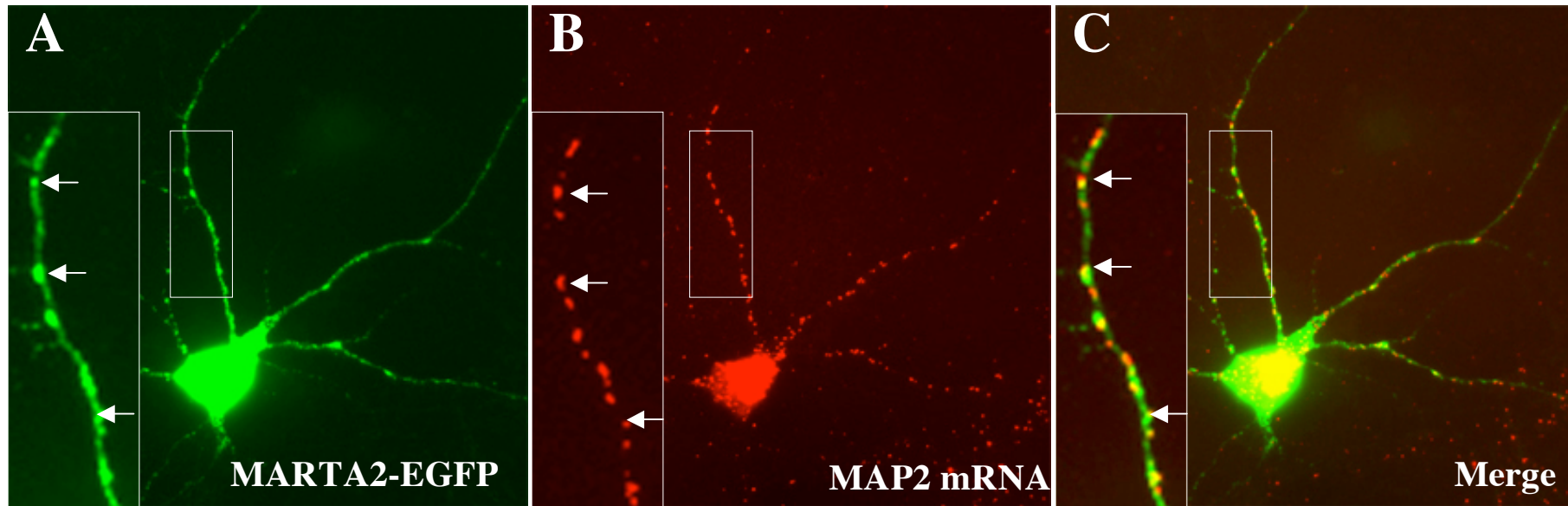


**FIGURE 15**

**Co-localization of recombinant MARTA2-EGFP with endogenous MAP2 mRNA in primary hippocampal neurons.** In one-week old hippocampal neurons expressing MARTA2-EGFP (A, polyclonal rabbit anti-GFP antibody and Alexa<sub>488</sub>-coupled goat secondary antibody) and endogenous MAP2 mRNAs (B, Cy3-coupled mouse digoxigenin antibody and Cy3-coupled goat secondary antibody) were visualized in a combined immunocytochemical and *in situ* hybridization assay. MARTA2-EGFP and MAP2 mRNAs extensively co-localized in granular structures distributed along dendrites (C; arrows). Scale bars: 25 μm.

### **3.3.2 Over-expression of truncated MARTA2 disrupts dendritic targeting of MAP2 mRNA.**

Albeit the co-localization of MARTA2 and MAP2 mRNA *in vivo*, the functional role of MARTA2 in dendritic MAP2 mRNA translocation remained unexplored. Therefore, to investigate a potential involvement of MARTA2 in dendritic MAP2 mRNA trafficking, a truncated version of the RNA-binding protein was expressed in primary neurons to test if it could dominantly inhibit MAP2 mRNA targeting *in vivo*. The rationale behind the dominant negative approach is that over-expression of a truncated version would sequester certain MARTA2 interaction partners that normally associate with parts of the protein that are missing in the truncated variant. These sequestered molecules can therefore no longer associate with MARTA2 to form a fully functional complex, thereby disrupting cellular processes in which MARTA2 participates. An EGFP-tagged recombinant MARTA2 isoform comprising of the four RNA-binding KH domains (MARTA2-KH-EGFP) was expressed in one-week old hippocampal neurons and the effect of the fusion protein on the distribution of endogenous MAP2 mRNA was analyzed two days later via *in situ* hybridization. In addition to the visualization of endogenous MAP2 transcripts, the transfected neurons were identified immunocytochemically using a GFP antibody. Furthermore, MAP2 protein was detected to highlight dendrites of primary neurons. It was assumed that while the truncated protein may still bind to the cis-acting MAP2-DTE, its ability to interact productively with other components of the mRNA localization machinery might be hampered. Indeed, in neurons expressing MARTA2-KH-EGFP, MAP2 mRNA granules were no longer detected in dendrites whereas RNA particles were still visible in the somata (figure 16 A, arrows). Yet in neighboring non-transfected neurons (figure 16,B, arrowheads), the

somatodendritic distribution of MAP2 mRNA granules was unaffected. Overall, MAP2 transcripts' levels in transfected neurons appeared to be somewhat reduced (figure 16,B). To test if this effect is attributed to the presence of the EGFP tag, EGFP alone was expressed in primary neurons followed by visualization of MAP2 mRNA granules. In contrast to MARTA2-KH-EGFP, over-expression of EGFP alone did not change the general distribution of dendritic MAP2 mRNA transcripts (figure 16, C and D) demonstrating that the disruption of MAP2 mRNA localization was due to the over-expression of the KH domains and was not influenced by the presence of the EGFP tag.

It is to be noted that KH domains are RNA binding domains. Hence, this raises the possibility that other RNA binding proteins may exert the same dominant negative effect on MAP2 mRNA granules similar to the KH domains of MARTA2. For this purpose, truncated *staufen2* (Tang *et al.* 2001) and cytoplasmic polyadenylation element binding protein (CPEB) (Huang *et al.* 2003) were expressed in primary neurons. Truncated *staufen2* that contains only the RNA binding domains (RBDs) was earlier shown to inhibit extrasomatic transport of polyadenylated mRNAs (Tang *et al.* 2001). CPEB on the other hand, was shown to facilitate transport of specific mRNAs, by binding to the *cis*-acting CPE present in specific dendritic mRNAs (Huang *et al.* 2003). The functional roles of truncated *staufen2*-EGFP and CPEB-EGFP described above makes them good controls for studying MARTA2's involvement in dendritic MAP2 mRNA targeting. Similar to cells expressing EGFP, truncated *staufen2*-EGFP (figure 16, E and F) or CPEB-EGFP (figure 16, G and H) expressing neurons showed dendritic MAP2 mRNA granules. The average density of MAP2 mRNA granules, which were observed in the proximal 60  $\mu\text{m}$  of the main dendritic branch was basically identical in cells over-

expressing EGFP ( $51.6 \pm 15.0$ ), truncated staufen2-EGFP ( $46.86 \pm 16.8$ ) or CPEB-EGFP ( $44.3 \pm 13.9$ ) and was only slightly reduced in comparison to non-transfected neurons ( $63 \pm 18.5$ ) (figure 17). On the other hand, these granules essentially disappeared from dendrites of MARTA2-KH-EGFP synthesizing neurons (0) (figure 17). The above results strongly emphasize that MARTA2 serves as a *trans*-acting factor in dendritic targeting of MAP2 mRNAs.

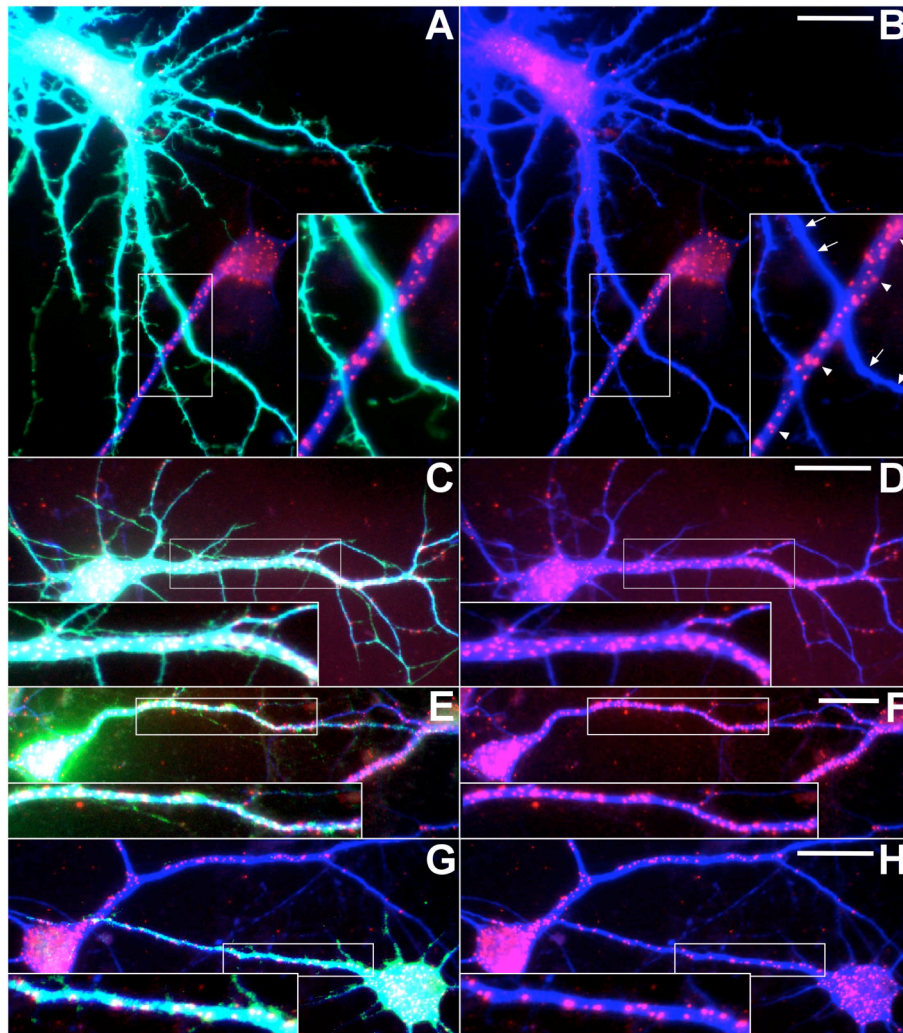


**FIGURE 16**

**Truncated MARTA2 disrupts dendritic targeting of endogenous MAP2 mRNA granules.** MARTA2-KH-EGFP (A, B), EGFP (C, D), truncated staufen2-EGFP (E, F) and CPEB-EGFP (G, H) were expressed in one week old hippocampal neurons. Two days after transfection, endogenous MAP2 transcripts were visualized by fluorescent *in situ* hybridization with Dig-Cy3-coupled antibodies (red). Endogenous MAP2 and various fusion proteins were detected via immunocytochemistry with anti-MAP2 and anti-GFP antibodies and secondary antibodies coupled to Marina Blue (blue) and Alexa<sub>488</sub> (green), respectively. Panels A, C, E and G are triple-stained images, in which transfected (turquoise) and non-transfected neurons (blue) are easily distinguished. Panels B, D, F and H are corresponding overlays of red and blue channels only, to allow clear visibility of MAP2 mRNA particles (magenta) along dendrites (blue) of transfected neurons. Higher magnification images of boxed areas are shown as insets to better visualize RNA granules distributed along MAP2-positive dendritic shafts. In non-transfected neurons, endogenous MAP2 mRNA granules are dispersed along dendritic shafts (B, arrowheads). However, upon the over-expression of truncated MARTA2, these transcript particles totally disappear from dendrites (B, arrows). In contrast, in neurons over-expressing EGFP (C, D), staufen2-EGFP (E, F), or CPEB-EGFP (G, H) MAP2 mRNA granules are normally distributed along dendrites. Micrographs were captured with a conventional fluorescence microscope. Scale bars: 25  $\mu$ m.

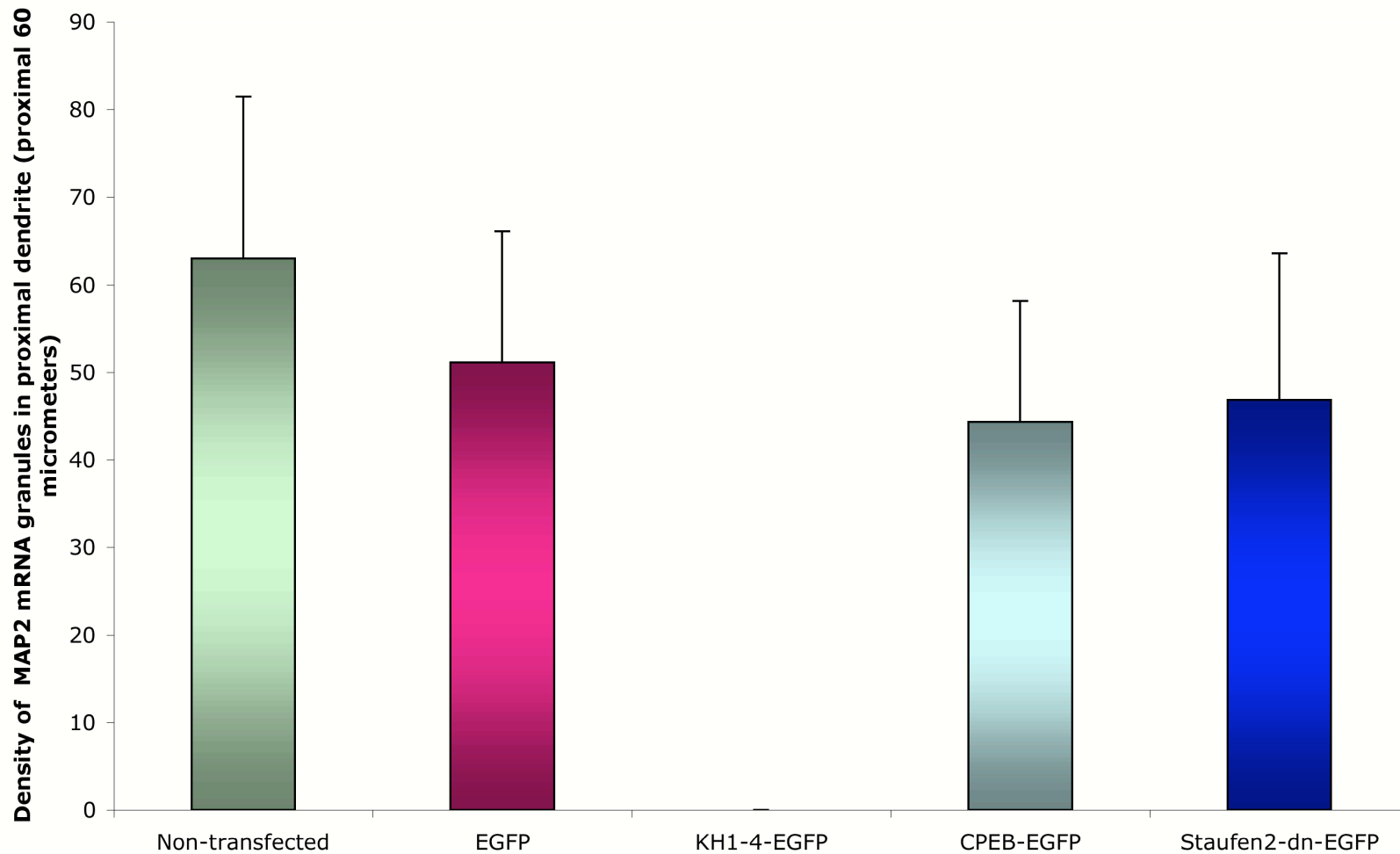


**FIGURE 17**

**Measurement of the amount of MAP2 mRNA granules in the proximal 60  $\mu\text{m}$  of the main dendritic branch.** Bar graph showing the average number (plus s.e.m) of endogenous MAP2 mRNA granules in non-transfected hippocampal neurons and in cells over-expressing different fusion proteins (as indicated below each bar). Granules were counted from two different experiments and 50 neurons were analyzed for each fusion protein.

### **3.3.3 MARTA2-KH-EGFP has no significant effect on the total mRNA pool.**

To test if over-expression of MARTA2-KH-EGFP somewhat specifically disrupts dendritic targeting of MAP2 transcripts or it may exhibit a more general effect on the subcellular distribution and stability of a larger pool of polyadenylated RNAs, the total mRNA pool of hippocampal neurons was visualized in neurons expressing the truncated protein. Interestingly, over-expression of truncated MARTA2-KH-EGFP, EGFP alone and truncated staufen2-EGFP (figure 18) did not drastically alter the subcellular distribution and concentration of the entire pool of polyadenylated mRNAs when compared to non-transfected neurons. An observation worth mentioning is that unlike previous reports from Tang *et al.* (2001), over-expression of truncated staufen2-EGFP did not reduce the pool of polyadenylated mRNAs in the above assay (figure 18, E, F). This difference between the above results and data from Tang *et al.* (2001) could be attributed to the methods employed. In contrast to the use of eukaryotic expression vectors and calcium phosphate transfection in the current study, Tang *et al.* (2001) used viral vectors to infect primary neurons. These methodological differences may lead to different levels of the fusion proteins in neurons and may thus affect the subsequent functional analysis of the protein. Nevertheless, the overall take home message from these experiments is that truncated MARTA2-KH-EGFP more or less selectively disrupts the dendritic targeting process of MAP2 mRNAs.

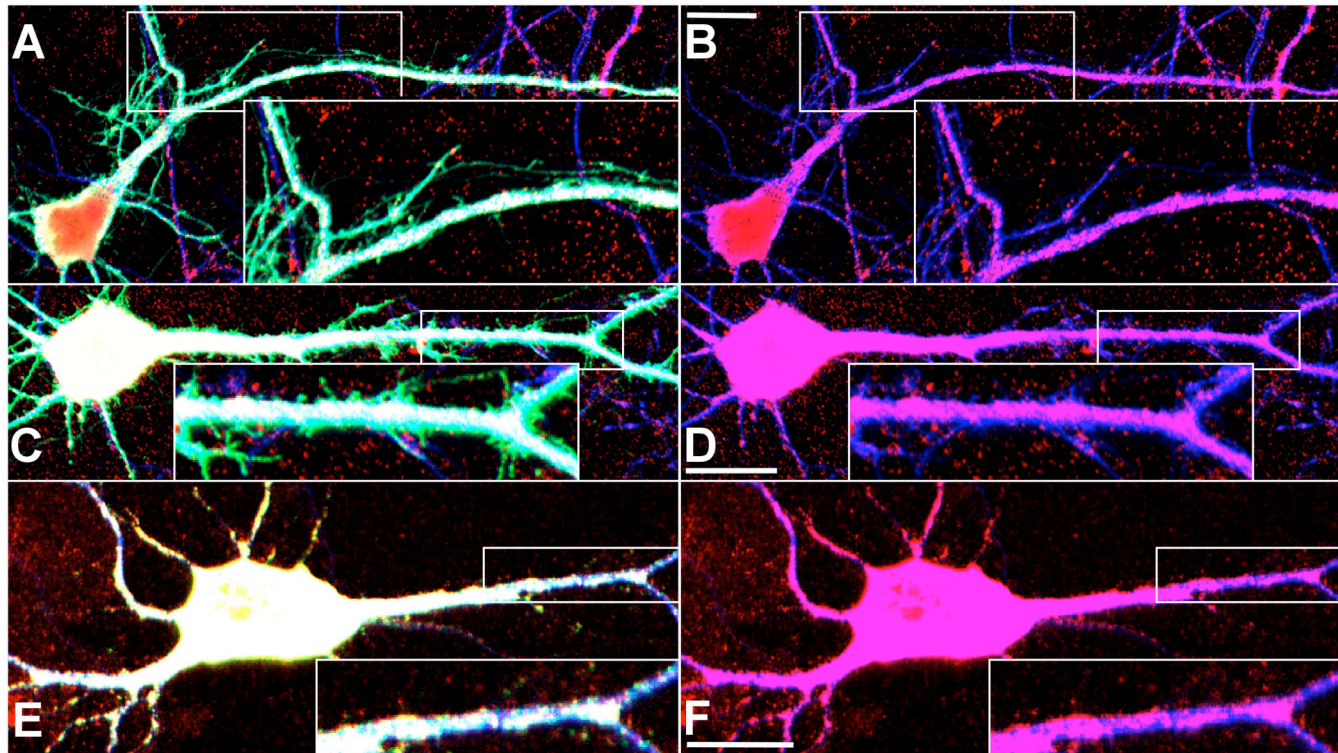


**FIGURE 18**

**Truncated MARTA2 does not generally interfere with the processing of polyadenylated mRNAs.** MARTA2-KH-EGFP (A, B), EGFP (C, D), and truncated stau2-EGFP (E, F) were expressed in one week old hippocampal neurons. After two days, polyadenylated transcripts (red), endogenous MAP2 (blue) and various fusion proteins (green) were detected. Panels A, C, and E are triple stained images, whereas panels B, D and F represent corresponding overlays of red and blue channels only. None of the recombinant proteins alters the concentration and distribution of polyadenylated mRNAs. Fluorescence micrographs were captured with a laser scanning microscope. Scale bars: 25  $\mu$ m.

### **3.3.4 Kinesin 1 mediates transport of MAP2 mRNA granules into dendrites.**

In many cases, RNA transport has been shown to depend on different motor proteins (Kinder *et al.* 2005). To investigate a possible role of motor proteins in extrasomatic MAP2 mRNA trafficking, a dominant negative version of kinesin I (dnKin-EGFP), or the dynein-associated protein dynamitin (Dyn-EGFP) (Burkhardt *et al.* 1997) was over-expressed in primary neurons. Dynamitin over-expression disrupts the function of cytoplasmic dynein (Burkhardt *et al.* 1997). Neurons expressing the recombinant motor proteins were analyzed two days after transfection for the distribution of endogenous MAP2 mRNA transcripts. In neurons expressing dnKin-EGFP, MAP2 mRNA granules were not detected in the dendritic compartment (figure 19, B). Dyn-EGFP or EGFP expressing neurons on the other hand, showed no significant difference in the distribution of the RNA particles in dendrites as compared to non-transfected neurons (figure 19, D and F). This observation was quantified by measuring the average amount of MAP2 mRNA granules in the proximal region of the main dendrite (figure 20). Quantification results show that the density of MAP2 mRNA transcripts in dendrites expressing Dyn-EGFP ( $61.2 \pm 17.6$ ) is essentially the same as in non-transfected neurons ( $63 \pm 18.5$ ) or in EGFP expressing neurons ( $51.5 \pm 15.0$ ) (figure 20). In contrast, the density of MAP2 mRNA in neurons expressing dn-Kin-EGFP is reduced to 0 (figure 20). Therefore, kinesin I, but not cytoplasmic dynein appears to be involved in the transport of MAP2 mRNA granules.

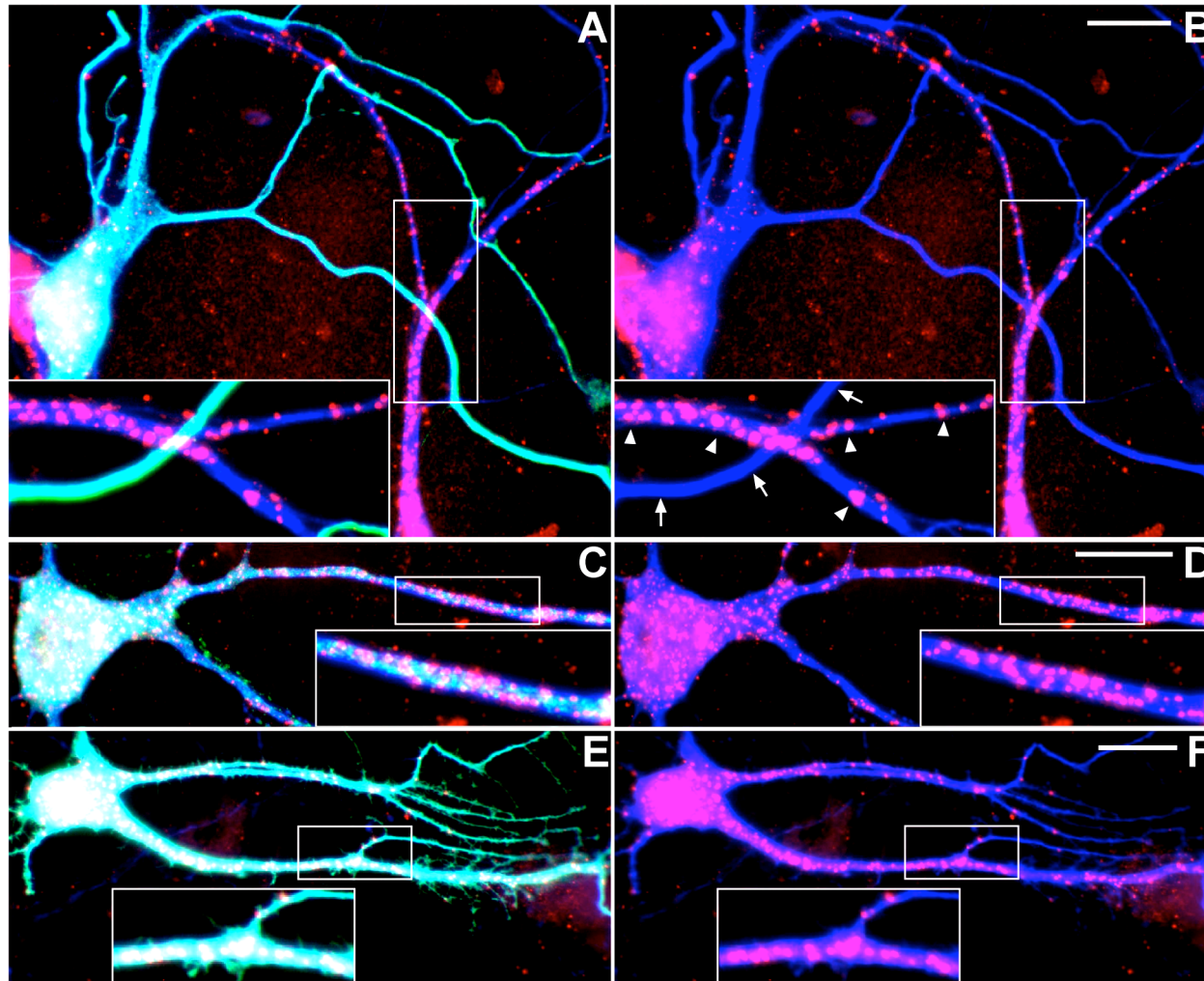


**FIGURE 19**

**Kinesin I mediates extrasomatic trafficking of endogenous MAP2 mRNA granules.** dn-Kin-EGFP (A, B), Dyn-EGFP (C, D), and EGFP (E, F) were expressed in one week old primary neurons and two days after transfection, endogenous MAP2 transcripts were visualized by fluorescence *in situ* hybridization with Cy3-coupled antibodies (red). Endogenous MAP2 and recombinant fusion proteins were immunostained with anti-MAP2 and anti-GFP antibodies and secondary antibodies coupled to Marina Blue (blue) and Alexa<sub>488</sub> (green), respectively. Panels A, C, E are triple stained images, whereas panels B, D, and F are corresponding merged red and blue channels only. In the latter, MAP2 mRNA particles (magenta) along dendrites (blue) are clearly visible. Higher magnification images of boxed areas are shown as insets. In non-transfected neurons, endogenous MAP2 mRNA granules are scattered along dendritic shafts (B, arrowheads). Over-expression of dn-Kin-EGFP disrupts dendritic targeting of these transcripts (B, arrows). In contrast, over-expression of Dyn-EGFP (C, D) or EGFP (E, F) does not interfere with the extrasomatic trafficking of mRNA granules. Micrographs were taken with a conventional fluorescence microscope. Scale bars: 25  $\mu$ m.

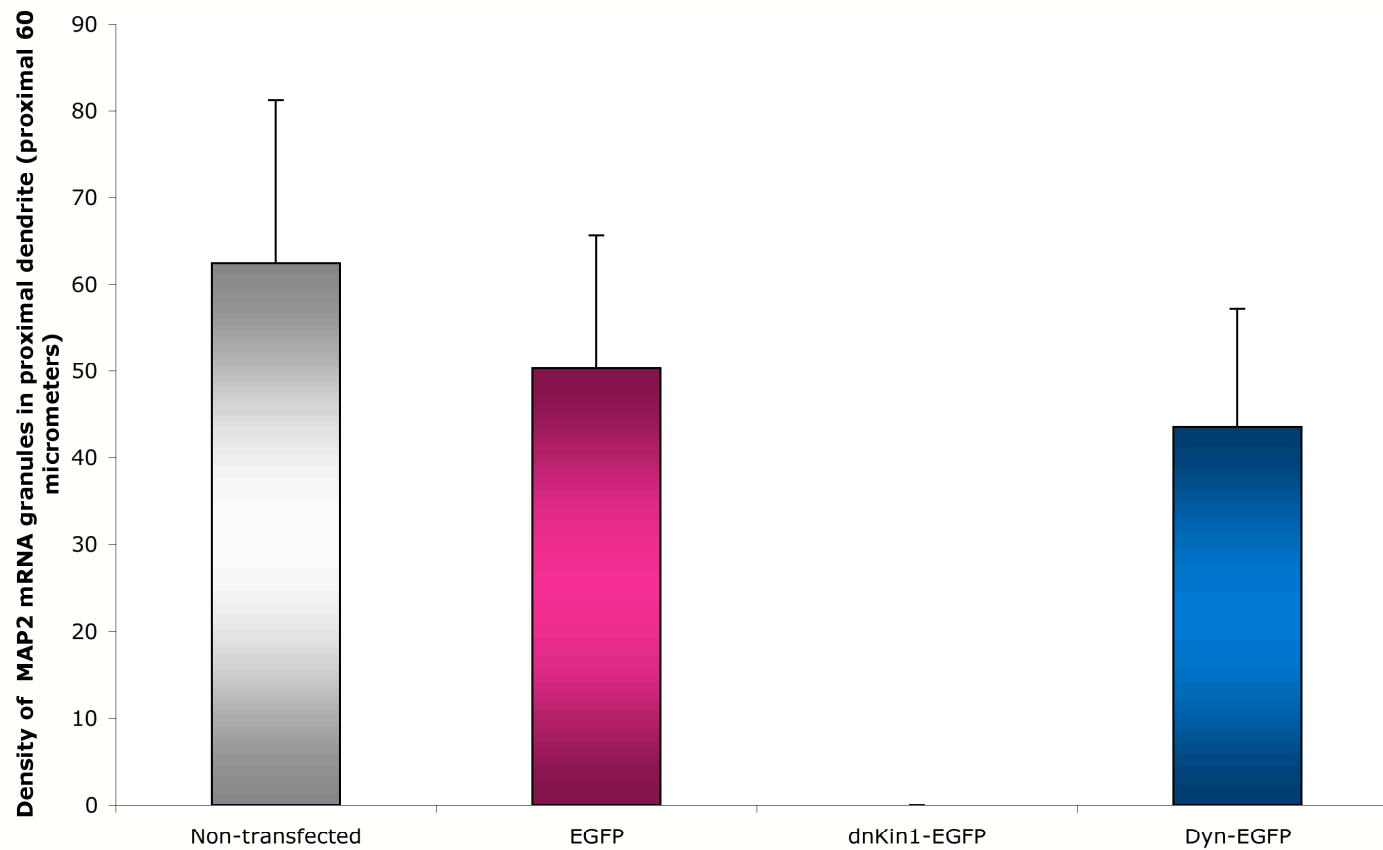


**FIGURE 20**

**Measurement of the amount of MAP2 mRNA granules in the proximal 60  $\mu$ m of the main dendritic branch.** Bar graph showing the average number (plus s.e.m) of endogenous MAP2 mRNA granules of non-transfected hippocampal neurons and cells over-expressing EGFP, dnKin1-EGFP or Dyn-EGFP as indicated below each bar. Granules were counted from two different experiments and 50 neurons were analyzed for each fusion protein.

## **CHAPTER 4: DISCUSSION**

In eukaryotic cells, two molecular mechanisms are implicated in differential protein localization. Selective protein sorting is one way of targeting proteins synthesized in the cytoplasm to the cellular sites where they are needed. Another means of protein sorting calls for post-transcriptional transport of messenger RNAs to the target site, followed by local and restricted translation (St Johnston 1995). In mammalian neurons for instance, a limited set of mRNA transcripts are targeted from the soma to the dendritic compartment (Job and Eberwine 2001). Transcripts encoding the cytoskeletal protein MAP2 were the first mRNAs that were found in dendrites (Garner et al. 1988). This discovery was particularly significant because MAP2 is a dendrite-specific protein stabilizing microtubules and participating in dendrite morphogenesis (Hirokawa 1994). In the current study, I attempted to answer a very basic question related to MAP2 mRNA transport in neurons. What are the molecules involved in delivering MAP2 mRNA from the soma to the dendrite of the neuron?

It is known that mRNAs during their travel are packaged into large transport particles or RNP complexes (Kindler *et al.* 2005). These complexes contain multiple mRNA molecules, RNA-binding proteins and translational machinery (Bassell *et al.* 1999) Although, radioactive *in situ* hybridization showed dendritic localization of MAP2 mRNA in primary neurons, visualization of the RNA as discrete transport granules was below the level of detection (Brukenstein *et al.* 1990; Kleiman *et al.* 1990). The FISH assay used in this study provided a higher spatial resolution and MAP2 mRNAs in the form of large distinct

granules, were seen along the dendritic shaft. These individual granules may indeed serve as transport units for the RNA.

During embryonic development in *Drosophila* and in *Xenopus*, mRNA localization is critical in defining cell polarity (Palachios and St. Johnston, 2001). Similarly, neurons being highly polarized cells may also employ mRNA sorting along with protein trafficking to establish their polarity. MAP2 being a dendritically localized protein has a strong influence on the organization of microtubules and stabilization of the dendritic cytoskeleton (Lewis *et al.* 1989; Weisshaar *et al.* 1992). MAP2 is also shown to support process outgrowth (Chen *et al.* 1992; Edson *et al.* 1993). Moreover, MAP2 deficient mice have shorter dendrites compared to wild type mice as tested in cultured hippocampal neurons and in intact hippocampal tissue (Harada *et al.* 2002). And finally, MAP2 suppression induced by siRNA in primary neurons results in severe defects in neurite outgrowth (Krichevsky and Kosik 2002). The above findings highlight the importance of MAP2 during neuronal morphogenesis. Data from previous as well as the current study show that MAP2 mRNA is dendritically localized. However, it is not clear as to how much dendritic mRNA transport contributes to neuronal differentiation. MAP2 mRNA localization was therefore examined in neurons at different developmental stages in culture. MAP2 mRNA granules were already seen in neurites at the inception of neuronal differentiation in culture underlining the importance of extrasomatic mRNA localization during neurogenesis. Along with mRNA transport, MAP2 protein localization also takes place in dendrites. In neurons derived from transgenic mice that express recombinant MAP2c isoform, the mRNA was seen only in the soma whereas the recombinant protein was detected in dendrites (Marsden *et al.* 1996). Hence, early sorting of MAP2 at the mRNA as well as at the protein

level appears to enhance the protein's contribution in neuronal differentiation and maturation.

The formation of RNP complexes is initiated by recognition of *cis*-acting RNA elements within the mRNA by *trans*-acting RNA-binding proteins (Kindler *et al.* 2005). A *cis*-acting 640-nucleotide spanning DTE that mediates dendritic transport of chimeric mRNAs was characterized in the 3'UTR of MAP2 mRNA (Blichenberg *et al.* 1999). Subsequently, two *trans*-acting factors called MARTA1 and MARTA2 that specifically interact with the MAP2-DTE were identified by UV cross-linking assays (Rehbein *et al.* 2000). MARTA1 was already affinity purified and characterized a few years ago (Rehbein *et al.* 2002). MARTA2 on the other hand, was only recently purified. Initial studies on MARTA2 by Western blot analysis showed that the protein is present in nuclear and polysome fractions but it is highly enriched in RSW fractions. The presence of MARTA2 in nuclear fractions suggests that the protein may associate with MAP2 mRNA in the nucleus and mediate its nuclear export. Studies in *Drosophila* embryo and in *Xenopus* oocyte have shown that nuclear events such as splicing and RNP formation are required to initiate cytoplasmic mRNA localization (Hachet and Ephrussi 2004; Kress *et al.* 2004). Moreover, a highly related family member MARTA1/ZBP2, which is predominantly present in the nucleus, interacts with  $\beta$ -actin mRNA and is involved in its cytoplasmic localization (Gu *et al.* 2002). The polysome fraction represents a mixture of polysomes and large RNP particles that have sedimentation properties similar to polysomes (Merrick 1992). Treatment of the polysome fraction with high salt concentration, dissociates its components. The resulting RSW fraction thus contains most of the molecules released from the disrupted complexes including components of the translational machinery (Merrick 1992). A

strong enrichment of MARTA2 in RSW fractions implies that the protein may be a part of an RNP complex and may even play a role in translational regulation. Moreover, the fact that MARTA2 contains four central RNA binding KH domains, gives the first indication that MARTA2 is involved in some aspect of mRNA processing. This hypothesis is further highlighted by the enrichment of the protein in RSW fractions. The RNA-binding protein Staufen well known for its role in mRNA localization (Roegiers and Jan, 2000) also regulates translation by potentially associating with ribosomes (Brendel *et al.* 2004). Based on the above evidence for MARTA2's distribution, a more precise speculation can be made suggesting that MARTA2 resides in granules representing RNP complexes, similar to those seen for MAP2 mRNA in neurons.

The above hypothesis is strongly supported by immunocytochemical and EM data which show that MARTA2 is somatodendritically distributed in the form of granules. Epitope-tagged MARTA2 also forms prominent granules in neuronal dendrites. The granular nature of the protein and its ability to bind RNA *in vitro* (Rehbein *et al.*, 2000) further emphasizes that MARTA2 forms an RNP complex. RNP particles often translocate along cytoskeletal filaments to reach their final destination (Hirokawa and Takemura, 2005). MARTA2 granules are also associated to the neuronal cytoskeleton as shown herein, thereby indicating that MARTA2 RNP particles which probably also contain MAP2 mRNA transcripts travel along the cell cytoskeleton.

It is clear by now that both MAP2 mRNA and MARTA2 form granules representing RNP complexes. However, despite the fact that MARTA2 binds the MAP2-DTE *in vitro* (Rehbein *et al.* 2000), it is not known if both molecules reside in the same RNP

complex *in vivo*. Co-localization experiments in primary neurons demonstrate that MAP2 mRNA co-localizes with endogenous and with recombinant MARTA2 in granules along dendrites. MARTA2 granules devoid of MAP2 mRNA were also observed, reflecting the possibility that MARTA2 may also form RNP complexes by interacting with other mRNA transcripts. These experiments accentuate the point that MARTA2 and MAP2 mRNA interact *in vivo*. These findings point towards the direction of MARTA2 acting as an *in vivo trans*-acting factor of the MAP2-DTE.

To test whether MARTA2 plays a role in dendritic MAP2 mRNA targeting, I used a dominant negative approach that involves over-expression of a truncated protein in a given cell system. It was hypothesized that MARTA2 contains RNA binding regions as well as “localizing” regions that mediate interactions for bringing the RNA and the protein to their final destination. Based on the above hypothesis, if a truncated protein comprising of only the RNA-binding KH domains of MARTA2 was over-expressed in neurons, the KH domains may recognize endogenous MAP2 mRNA however other interactions of MARTA2 normally mediated via its N- and C-terminal domains would not occur with the truncated protein. If true, incomplete RNP particles would be formed with MAP2 mRNA. These incomplete RNP complexes may not be able to perform its normal cellular function such as dendritic MAP2 mRNA transport and hence the RNP complex will remain captivated in the soma. The dominant negative approach was successfully used for studying  $\beta$ -actin mRNA localization in neurons as well as in fibroblasts, mediated by its two *trans*-acting proteins ZBP1 and ZBP2 (Gu *et al.* 2002; Farina *et al.* 2003). Similarly, in *Xenopus* oocytes, a functional role for Staufen was revealed through expression of a dominant-negative version of the *Xenopus* homolog (XStau) that blocked the

localization of Vg1 RNA *in vivo* (Yoon and Mowry 2004). To investigate a potential dominant-negative effect of truncated MARTA2, EGFP-fused KH domains of MARTA2 (MARTA2-KH-EGFP) were over-expressed in neurons and the distribution of endogenous MAP2 mRNA granules was examined. MARTA2-KH-EGFP indeed caused a dominant-negative effect in neurons as MAP2 mRNA granules were no longer distributed along dendrites. This effect was not mainly due to the EGFP-tag as over-expression of EGFP alone showed only a slight reduction in the dendritic distribution of MAP2 mRNA in comparison to non-transfected neurons. Similarly, extrasomatic MAP2 mRNA transport mediated by other RNA-binding proteins or RNA binding domains was investigated. Over-expression of the RNA-binding protein CPEB (Huang *et al.* 2003), and an incomplete version of Staufen2 containing only the RBD-domains (Tang *et al.* 2001), had no profound influence on dendritic MAP2 mRNA trafficking. Hence, MARTA2 appears to play a central role in extrasomatic trafficking of MAP2 transcripts. Interestingly, the dominant negative effect seen for cytoplasmic  $\beta$ -actin mRNA localization was also induced by the over-expression of the KH domains of either ZBP1 and ZBP2 (Gu *et al.* 2002; Farina *et al.* 2003). Thus, different RNA binding proteins seem to be involved in cytoplasmic translocation of distinct mRNAs. Although, the dominant negative analysis is a first step in elucidating the role of MARTA2 in MAP2 mRNA localization, a more direct approach such as siRNA mediated knock-down of MARTA2 in primary neurons would further consolidate the role of MARTA2 as a *trans*-acting factor for extrasomatic MAP2 mRNA localization.

Co-localization experiments show that MARTA2 is present in other RNP complexes besides the ones containing MAP2 mRNA. Thus, MARTA2 may also bind to other mRNA transcripts

via its KH domains. This concept raises the possibility that over-expression of the KH domains may not specifically inhibit only MAP2 mRNA localization but also affect the distribution of other neuronal mRNAs. Hence, the effect of over-expression of MARTA2-KH-EGFP on the entire pool of polyadenylated mRNAs in neurons was examined. Over-expression of neither truncated MARTA2 nor EGFP and truncated staufen-2 significantly altered the subcellular distribution and concentration of the total polyadenylated mRNA pool. The result obtained indicates that MARTA2 most likely does not influence the transport of a majority of neuronal transcripts *in vivo*, however the protein may still bind to other RNA targets besides MAP2 mRNA. *In vitro*, it is known that MARTA2 does not bind to dendritically localized vasopressin and arg 3.1 mRNAs, nor does it bind to the DTE of  $\alpha$ -CaMKII (Rehbein *et al.* 2000). It would be interesting to identify other RNA targets of MARTA2. Hence, even though MARTA2 plays a central role in the dendritic translocation of MAP2 mRNAs, it may still bind to other messenger transcripts and participate in different mRNA processing mechanisms.

MARTA2 functioning as a *trans*-acting factor in MAP2 mRNA transport is just one aspect of mRNA localization. mRNA transport by itself is a complex multi-step process requiring specific set of RNA binding proteins at each step. Newly accumulated evidences from *Drosophila* embryos and *Xenopus* oocytes reveal that distinct nuclear and cytoplasmic steps are required for proper localization of mRNA transcripts (Hatchet and Euphrassi, 2004; Kress *et al.* 2004). The splicing of *Drosophila*'s oskar mRNA mediated by the components of the exon junction complex namely Y14/Tsunagi and Mago nashi, regulates RNP complex assembly in the nucleus, followed by the organization of the mRNA's cytoplasmic localization (Hatchet and Euphrassi, 2004). Assembly of RNP complexes in the

nucleus also occurs in *Xenopus* oocytes. Vg1 mRNA localization is initiated by the mRNA forming an RNP complex with two RNA binding nucleocytoplasmic shuttling proteins namely hnRNP I and Vg1 RBP (Kress *et al.* 2004). Both proteins bind to Vg1 mRNA in the nucleus and remain in complex with the RNA even after export into the cytoplasm. Within the cytoplasm, the pre-existing RNP complex gets remodeled by recruitment of additional factors such as XStau (Kress *et al.* 2004). Hence, mRNA targeting is carried out stepwise wherein an RNA, from the time of its transcription in the nucleus to the point when it reaches its final destination, enlists a set of RNA binding proteins that function in a sequentially orchestrated manner (Kindler *et al.* 2005).

Cytoplasmic RNA particles in eukaryotic cells typically move along cytoskeletal filaments to reach their final destination (Kindler *et al.* 2005). Translocation of mRNA granules was visualized in live neurons using the membrane-permeable dye SYTO 14 that allows detection of polyadenylated mRNAs (Knowles *et al.* 1996). Transport of mRNA granules was blocked when neurons were treated with microtubule-disrupting drugs (Knowles *et al.* 1996). While the transport of  $\beta$ -actin mRNA in fibroblasts is microfilament-dependent, the same mRNA is targeted into developing neurites and growth cones in culture via microtubules (Bassell *et al.* 1998). Hence in neurons, RNP granules embark on microtubules to start their journey into dendrites. During their travel, molecular motors facilitate RNPs to traverse long distances along the microtubule tracks (Guzik and Goldstein, 2004). Like most RNP complexes, it was speculated that MAP2 mRNA complexes may also associate with motor proteins. Possible involvement of conventional kinesin and/or dynein was therefore investigated. Over-expression of truncated conventional kinesin (dnKin1-EGFP) consisting of

only the motor domain disrupted MAP2 mRNA targeting in dendrites. In contrast, over-expression of dynamitin-EGFP that causes an impairment of cytoplasmic dynein function (Burkhardt et al. 1997) did not interfere with extrasomatic MAP2 transcript trafficking. Thus, kinesin1 appears to mediate dendritic MAP2 mRNA targeting.

In conclusion, my data show that in neurons, MARTA2 acts as a *trans*-acting factor in the extrasomatic trafficking of MAP2 mRNA in the form of RNP complexes. The involvement of conventional kinesin in mediating the localization of MAP2 mRNA probably by its association with MARTA2 RNPs, takes this study a step further in understanding the mechanisms that regulate mRNA transport.

**CHAPTER 5: SUMMARY**

Cytoplasmic mRNA localization is one important mechanism that contributes to differential protein sorting in eukaryotic cells. In mammalian neurons, extrasomatic trafficking of a distinct subset of mRNAs occurs to regulate *de novo* synthesis of proteins at a specific cellular site. One such mRNA that is dendritically localized is the mRNA encoding microtubule-associated protein 2 (MAP2). Typical of localized mRNAs, MAP2 mRNA contains a *cis*-acting dendritic targeting element (DTE) in its 3' untranslated region (3'UTR) that is recognized by two *trans*-acting factors namely MARTA1 and the recently purified MARTA2. The current study puts the spotlight on MAP2 mRNA and its dendritic targeting mediated by MARTA2.

In general, mRNA transcripts are localized in the form of ribonucleoprotein (RNP) granules, which appear to be an assortment of multiple mRNA molecules associated with proteins and components of the translational machinery that traverse along cytoskeletal filaments. Likewise, data obtained from the current study demonstrates that MAP2 mRNA in primary neurons also resides in granules along dendritic shafts that may represent RNP complexes. MAP2 mRNA's *trans*-acting factor MARTA2 is the rat ortholog of human FBP3, which contains four central KH domains involved in RNA/DNA binding. Similar to MAP2 mRNA, I found that MARTA2 also has a somatodendritic granular distribution in primary neurons. In addition, the protein is associated with the neuronal cytoskeleton and is concentrated in cell fractions enriched for RNP particles. These findings strongly support the presence of MARTA2 in an RNP complex. Moreover, colocalization studies show that MAP2 mRNA and MARTA2 are present in the same granules *in vivo*.

Since MARTA2 is present in MAP2 mRNA granules, is it a key player in the dendritic trafficking of the mRNA? To address

this question, truncated MARTA2 containing only the KH domains was over-expressed in neurons. Truncated MARTA2 indeed exerts a strong dominant-negative effect as it completely disrupts dendritic targeting of endogenous MAP2 mRNAs, a result that is not caused by two other RNA-binding proteins Staufen2 and CPEB. The dominant-negative effect induced by truncated MARTA2 appears to be more or less selective for MAP2 mRNA as the incomplete protein does not significantly alter the concentration and subcellular distribution of the entire neuronal pool of polyadenylated mRNAs. Along with truncated MARTA2, a dominant negative version of conventional kinesin also inhibits extrasomatic trafficking of MAP2 mRNA granules. In contrast, over-expression of dynamitin which hinders cytoplasmic dynein function, had no effect on the mRNA particles. Hence, in a nutshell, my data demonstrate that MARTA2 acts as an important *trans*-acting factor that is involved in kinesin-dependent dendritic MAP2 mRNA targeting.

Aranda-Abreu, G. E., L. Behar, et al. (1999). "Embryonic lethal abnormal vision-like RNA-binding proteins regulate neurite outgrowth and tau expression in PC12 cells." J Neurosci **19**(16): 6907-17.

Aronov, S., G. Aranda, et al. (2002). "Visualization of translated tau protein in the axons of neuronal P19 cells and characterization of tau RNP granules." J Cell Sci **115**(Pt 19): 3817-27.

Banker, G. and K. Goslin (1988). "Developments in neuronal cell culture." Nature **336**(6195): 185-6.

Bashirullah, A., R. L. Cooperstock, et al. (1998). "RNA localization in development." Annu. Rev. Biochem. **67**: 335-94.

Bassell, G. J. and S. Kelic (2004). "Binding proteins for mRNA localization and local translation, and their dysfunction in genetic neurological disease." Curr Opin Neurobiol **14**(5): 574-81.

Bassell, G. J., Y. Oleynikov, et al. (1999). "The travels of mRNAs through all cells large and small." Faseb J. **13**(3): 447-54.

Bassell, G. J., H. Zhang, et al. (1998). "Sorting of beta-actin mRNA and protein to neurites and growth cones in culture." J. Neurosci. **18**(1): 251-65.

Berleth, T., M. Burri, et al. (1988). "The role of localization of bicoid RNA in organizing the anterior pattern of the Drosophila embryo." Embo J **7**(6): 1749-56.

Blichenberg, A., M. Rehbein, et al. (2001). "Identification of a *cis*-acting dendritic targeting element in the mRNA encoding the alpha subunit of Ca<sup>2+</sup>/calmodulin-dependent protein kinase II." Eur J Neurosci **13**(10): 1881-8.

**Blichenberg, A., B. Schwanke,** et al. (1999). "Identification of a *cis*-acting dendritic targeting element in MAP2 mRNAs." J Neurosci **19**(20): 8818-29.

- Bodian, D. (1965). "A Suggestive Relationship of Nerve Cell Rna with Specific Synaptic Sites." Proc Natl Acad Sci U S A **53**: 418-25.
- Braddock, D. T., J. M. Louis, et al. (2002). "Structure and dynamics of KH domains from FBP bound to single-stranded DNA." Nature **415**(6875): 1051-6.
- Brendel, C., M. Rehbein, et al. (2004). "Characterization of Staufen 1 ribonucleoprotein complexes." Biochem J Pt.
- Bruckenstein, D. A., P. J. Lein, et al. (1990). "Distinct spatial localization of specific mRNAs in cultured sympathetic neurons." Neuron **5**(6): 809-19.
- Burkhardt, J. K., C. J. Echeverri, et al. (1997). "Overexpression of the dynamitin (p50) subunit of the dynactin complex disrupts dynein-dependent maintenance of membrane organelle distribution." J Cell Biol **139**(2): 469-84.
- Caceres, A., G. Banker, et al. (1984). "MAP2 is localized to the dendrites of hippocampal neurons which develop in culture." Brain Res **315**(2): 314-8.
- Caceres, A., L. I. Binder, et al. (1984). "Differential subcellular localization of tubulin and the microtubule-associated protein MAP2 in brain tissue as revealed by immunocytochemistry with monoclonal hybridoma antibodies." J Neurosci **4**(2): 394-410.
- Carson, J. H., H. Cui, et al. (2001). "RNA trafficking in oligodendrocytes." Results Probl Cell Differ **34**: 69-81.
- Chen, J., Y. Kanai, et al. (1992). "Projection domains of MAP2 and tau determine spacings between microtubules in dendrites and axons." Nature **360**(6405): 674-7.
- Davis-Smyth, T., R. C. Duncan, et al. (1996). "The far upstream element-binding proteins comprise an ancient family of single-

strand DNA-binding transactivators." J Biol Chem **271**(49): 31679-87.

Deshler, J. O., M. I. Highett, et al. (1997). "Localization of *Xenopus* Vg1 mRNA by Vera protein and the endoplasmic reticulum." Science **276**(5315): 1128-1131.

Duchaine, T. F., I. Hemraj, et al. (2002). "Staufen2 isoforms localize to the somatodendritic domain of neurons and interact with different organelles." J Cell Sci **115**(Pt 16): 3285-95.

Duncan, R., L. Bazar, et al. (1994). "A sequence-specific, single-strand binding protein activates the far upstream element of *c-myc* and defines a new DNA-binding motif." Genes Dev **8**(4): 465-80.

Eberwine, J., B. Belt, et al. (2002). "Analysis of subcellularly localized mRNAs using in situ hybridization, mRNA amplification, and expression profiling." Neurochem Res **27**(10): 1065-77.

Edson, K., B. Weisshaar, et al. (1993). "Actin depolymerisation induces process formation on MAP2-transfected non-neuronal cells." Development **117**(2): 689-700.

Eom, T., L. N. Antar, et al. (2003). "Localization of a beta-actin messenger ribonucleoprotein complex with zipcode-binding protein modulates the density of dendritic filopodia and filopodial synapses." J Neurosci **23**(32): 10433-44.

Farina, K. L., S. Huttelmaier, et al. (2003). "Two ZBP1 KH domains facilitate beta-actin mRNA localization, granule formation, and cytoskeletal attachment." J Cell Biol **160**(1): 77-87.

Frigerio, G., M. Burri, et al. (1986). "Structure of the segmentation gene paired and the *Drosophila* PRD gene set as part of a gene network." Cell **47**(5): 735-46.

Garner, C. C., R. P. Tucker, et al. (1988). "Selective localization of messenger RNA for cytoskeletal protein MAP2 in dendrites." Nature **336**(6200): 674-7.

Gherzi, R., K. Y. Lee, et al. (2004). "A KH domain RNA binding protein, KSRP, promotes ARE-directed mRNA turnover by recruiting the degradation machinery." Mol Cell **14**(5): 571-83.

Goedert, M., R. A. Crowther, et al. (1991). "Molecular characterization of microtubule-associated proteins tau and MAP2." Trends Neurosci **14**(5): 193-9.

Goslin, K. and G. Banker (1989). "Experimental observations on the development of polarity by hippocampal neurons in culture." J Cell Biol **108**(4): 1507-16.

Goslin, K., D. J. Schreyer, et al. (1990). "Changes in the distribution of GAP-43 during the development of neuronal polarity." J Neurosci **10**(2): 588-602.

Gu, W., F. Pan, et al. (2002). "A predominantly nuclear protein affecting cytoplasmic localization of beta-actin mRNA in fibroblasts and neurons." J Cell Biol **156**(1): 41-51.

Guzik, B. W. and L. S. Goldstein (2004). "Microtubule-dependent transport in neurons: steps towards an understanding of regulation, function and dysfunction." Curr Opin Cell Biol **16**(4): 443-50.

Hachet, O. and A. Ephrussi (2004). "Splicing of oskar RNA in the nucleus is coupled to its cytoplasmic localization." Nature **428**(6986): 959-63.

Harada, A., J. Teng, et al. (2002). "MAP2 is required for dendrite elongation, PKA anchoring in dendrites, and proper PKA signal transduction." J Cell Biol **158**(3): 541-9.

Hirokawa, N. (1994). "Microtubule organization and dynamics dependent on microtubule-associated proteins." Curr Opin Cell Biol **6**(1): 74-81.

Hirokawa, N. and R. Takemura (2005). "Molecular motors and mechanisms of directional transport in neurons." Nat Rev Neurosci **6**(3): 201-14.

Huang, Y. S., J. H. Carson, et al. (2003). "Facilitation of dendritic mRNA transport by CPEB." Genes Dev **17**(5): 638-53.

Job, C. and J. Eberwine (2001). "Localization and translation of mRNA in dendrites and axons." Nat. Rev. Neurosci. **2**(12): 889-98.

Kanai, Y., N. Dohmae, et al. (2004). "Kinesin transports RNA: isolation and characterization of an RNA-transporting granule." Neuron **43**(4): 513-25.

Kindler, S., H. Wang, et al. (2005). "RNA Transport and Local Control of Translation." Annu Rev Cell Dev Biol **21**: 223-245.

Kislauskis, E. H., X. Zhu, et al. (1994). "Sequences responsible for intracellular localization of beta-actin messenger RNA also affect cell phenotype." J Cell Biol **127**(2): 441-51.

Kleiman, R., G. Banker, et al. (1990). "Differential subcellular localization of particular mRNAs in hippocampal neurons in culture." Neuron **5**(6): 821-30.

Kloc, M., N. R. Zearfoss, et al. (2002). "Mechanisms of subcellular mRNA localization." Cell **108**(4): 533-44.

Knowles, R. B., J. H. Sabry, et al. (1996). "Translocation of RNA granules in living neurons." J. Neurosci. **16**(24): 7812-20.

Kress, T. L., Y. J. Yoon, et al. (2004). "Nuclear RNP complex assembly initiates cytoplasmic RNA localization." J Cell Biol **165**(2): 203-11.

Krichevsky, A. M. and K. S. Kosik (2002). "RNAi functions in cultured mammalian neurons." Proc Natl Acad Sci U S A **99**(18): 11926-9.

Laemmli, U. K. (1970). "Cleavage of structural proteins during the assembly of the head of bacteriophage T4." Nature **227**(5259): 680-5.

Lewis, S. A., I. E. Ivanov, et al. (1989). "Organization of microtubules in dendrites and axons is determined by a short hydrophobic zipper in microtubule-associated proteins MAP2 and tau." Nature **342**(6249): 498-505.

Long, R. M., R. H. Singer, et al. (1997). "Mating type switching in yeast controlled by asymmetric localization of ASH1 mRNA." Science **277**(5324): 383-7.

Marsden, K. M., T. Doll, et al. (1996). "Transgenic expression of embryonic MAP2 in adult mouse brain: implications for neuronal polarization." J Neurosci **16**(10): 3265-73.

Matus, A. (1994). "Stiff microtubules and neuronal morphology." Trends Neurosci **17**(1): 19-22.

Merrick, W. C. (1992). "Mechanism and regulation of eukaryotic protein synthesis." Microbiol Rev **56**(2): 291-315.

Min, H., C. W. Turck, et al. (1997). "A new regulatory protein, KSRP, mediates exon inclusion through an intronic splicing enhancer." Genes Dev **11**(8): 1023-36.

Monshausen, M., U. Putz, et al. (2001). "Two rat brain Staufen isoforms differentially bind RNA." J Neurochem **76**(1): 155-165.

Monshausen, M., M. Rehbein, et al. (2002). "The RNA-binding protein Staufen from rat brain interacts with protein phosphatase-1." J Neurochem **81**(3): 557-64.

Mouland, A. J., H. Xu, et al. (2001). "RNA trafficking signals in human immunodeficiency virus type 1." Mol Cell Biol **21**(6): 2133-43.

Mowry, K. L. and D. A. Melton (1992). "Vegetal messenger RNA localization directed by a 240-nt RNA sequence element in *Xenopus* oocytes." Science **255**: 991-994.

Palacios, I. M. and D. St Johnston (2001). "Getting the message across: the intracellular localization of mRNAs in higher eukaryotes." Annu Rev Cell Dev Biol **17**: 569-614.

Rebagliati, M. R., D. L. Weeks, et al. (1985). "Identification and cloning of localized maternal RNAs from *Xenopus* eggs." Cell **42**(3): 769-77.

Rehbein, M., S. Kindler, et al. (2000). "Two trans-acting rat-brain proteins, MARTA1 and MARTA2, interact specifically with the dendritic targeting element in MAP2 mRNAs." Brain Res Mol Brain Res **79**(1-2): 192-201.

Rehbein, M., K. Wege, et al. (2002). "Molecular characterization of MARTA1, a protein interacting with the dendritic targeting element of MAP2 mRNAs." J Neurochem **82**(5): 1039-46.

Roegiers, F. and Y. N. Jan (2000). "Staufen: a common component of mRNA transport in oocytes and neurons?" Trends Cell Biol **10**(6): 220-224.

Ross, A. F., Y. Oleynikov, et al. (1997). "Characterization of a beta-actin mRNA zipcode-binding protein." Mol Cell Biol **17**(4): 2158-65.

Sambrook, J., E. F. Fritsch, et al. (1989). Molecular Cloning: A Laboratory Manual. Cold Spring Harbor, NY, Cold Spring Harbor Laboratory Press.

Sanger, F., S. Nicklen, et al. (1977). "DNA sequencing with chain-terminating inhibitors." Proc Natl Acad Sci U S A **74**(12): 5463-7.

Siomi, H., M. Choi, et al. (1994). "Essential role for KH domains in RNA binding: impaired RNA binding by a mutation in the KH domain of FMR1 that causes fragile X syndrome." Cell **77**(1): 33-9.

St Johnston, D. (1995). "The intracellular localization of messenger RNAs." Cell **81**(2): 161-70.

Steward, O. and W. B. Levy (1982). "Preferential localization of polyribosomes under the base of dendritic spines in granule cells of the dentate gyrus." J Neurosci **2**(3): 284-291.

Tang, S. J., D. Meulemans, et al. (2001). "A role for a rat homolog of staufen in the transport of RNA to neuronal dendrites." Neuron **32**(3): 463-75.

Tiruchinapalli, D. M., Y. Oleynikov, et al. (2003). "Activity-dependent trafficking and dynamic localization of zipcode binding protein 1 and beta-actin mRNA in dendrites and spines of hippocampal neurons." J Neurosci **23**(8): 3251-61.

Weisshaar, B., T. Doll, et al. (1992). "Reorganisation of the microtubular cytoskeleton by embryonic microtubule-associated protein 2 (MAP2c)." Development **116**(4): 1151-61.

Yoon, Y. J. and K. L. Mowry (2004). "Xenopus Staufien is a component of a ribonucleoprotein complex containing Vg1 RNA and kinesin." Development **131**(13): 3035-45.

Zhang, H. L., T. Eom, et al. (2001). "Neurotrophin-induced transport of a beta-actin mRNP complex increases beta-actin levels and stimulates growth cone motility." Neuron **31**(2): 261-75.

Zivraj, K., M. Rehbein, et al. (2005). "RNA-binding protein MARTA2 regulates dendritic MAP2 mRNA targeting." (in preparation).

## **Erklärung**

Hiermit versichere ich, dass ich die vorliegende Arbeit selbständig und ohne fremde Hilfe verfasst, keine anderen als die angegebenen Hilfsmittel benutzt und die den verwendeten Werken wörtlich oder inhaltlich entnommenen Stellen als solche kenntlich gemacht habe.

Ferner versichere ich, dass ich mich zu keiner Zeit anderweitig um Erlangung des Doktorgrades beworben habe.

Hamburg, September 2005

Krishna H. Zivraj

## **Academic Profile**

*University Hospital Eppendorf*, Hamburg, Germany, November 2002 to date (Expected date of completion – October 2005)

- PhD student in Dr. Stefan Kindler's lab.
- Thesis title- Regulation of dendritic MAP2 mRNA targeting by MARTA2 in *Rattus norvegicus*.

*Centre Médical Universitaire, University of Geneva*, Geneva, Switzerland, October 2001- October 2002

- Diplomat/ Master's student under the supervision of Prof. Ivan Rodriguez at the department of Zoology and Animal Biology, University of Geneva, Geneva, Switzerland.

Thesis title- Regulation of the vomeronasal V1R gene family in mice.

*Albright College*, Reading Pennsylvania, USA, August 1997- May 2000.

- Bachelor of Science in Biochemistry and French.

## **Scholarships and Prizes**

- **Recipient, Pre-Doctoral Travel Award** to attend the 44<sup>th</sup> American Society for Cell Biology (ASCB) Annual Meeting, Washington D.C, U.S.A, December 4-8, 2004.
- **International Student Scholarship**, Albright College, USA.
- **Recipient, Who's Who Among Students in American Universities & Colleges Award**, 1999-2000, Albright College, USA

## **Conferences and Meetings:**

- **18<sup>th</sup> National Meeting, British Neuroscience Association**, Brighton, England. April 3<sup>rd</sup>- 6<sup>th</sup>, 2005. Poster title- *Dendritic MAP2 mRNA targeting in rat neurons*.
- **44<sup>th</sup> American Society for Cell Biology (ASCB) Annual Meeting**, Washington D.C, U.S.A, December 4-8, 2004. Poster title- *Dendritic MAP2 mRNA targeting in rat neurons*.
- **24<sup>th</sup> Blankenese Conference- From Genes to Therapy**, Hamburg-Blankenese, Germany, May 16-20, 2004. Poster title- *Dendritic MAP2 mRNA targeting in rat neurons*.
- **Zentrum für Molekulare Neurobiologie, Hamburg (ZMNH) Retreat**, Bad Segeburg, Germany, April 28-29, 2004. Poster title- *Dendritic MAP2 mRNA targeting in rat neurons*.
- **Attended the International Symposium of the DFG research group 'Complex RNA- protein interactions in the maturation and function of eukaryotic mRNA'**, Gottingen, Germany, September 17-20, 2003.
- **Attended the 23th Blankenese Conference- Learning at/from the Synapse**, Hamburg- Blankenese, Germany, May 8-12, 2003.

## **Publication:**

***Manuscript in preparation- The RNA Binding Protein MARTA2 Regulates Dendritic MAP2 RNA Targeting.***

Krishna H. Zivraj, Monika Rehbein, Friedrich Buck, Michaela Schweizer, Dietmar Richter and Stefan Kindler.